Vibration Control of Horizontally Supported Jeffcott-Rotor System Utilizing PIRC-controller (2023)

Osama M. Omara, M. Sayed, and Nasser. A. Saeed

Abstract— **This paper is devoted to investigate the nonlinear vibration control of a horizontally supported rotor system governed by two coupled second-order differential equations having both quadratic and cubic nonlinearities. A combination of the proportional controller and the integral resonant controller is employed to suppress the undesired lateral vibration of the considered rotor system. In addition, an 8-pole active-magnetic-bearing is utilized as an active actuator through which the control signal will be applied on the rotor system in the form of electromagnetic attractive forces. Based on the proposed control strategy, the whole system mathematical model has been established as a nonlinear two-degree-of-freedom system coupled to two first-order differential equations. Then, the multiple scales perturbation method has been applied to obtain an analytical solution for the obtained mathematical model up to the second-order approximation. Using the derived analytical solution, the influence of the different control gains on the system vibration amplitudes has been explored in terms of different bifurcation diagrams. The obtained results showed that the proposed control method can mitigate the rotor undesired vibrations close to zero regardless of the excitation force amplitude. Moreover, numerical validation for all obtained analytical results has been performed using the Runge-Kutta algorithm, where an excellent agreement between the analytical and numerical results is demonstrated.**

Keywords— ***Nonlinear vibration, proportional controller, integral resonant controller, perturbation method, 8-pole active-magnetic-bearing, Jeffcott rotor.***

I. INTRODUCTION

ROTATING machines' vibration is one of the biggest problems that has drawn the attention of scientists and engineers worldwide. Nonlinear vibrations arise in rotating machines as a result of many different reasons, which are: the imbalance of the rotating shafts, looseness of the bearings, bearings clearance, crack propagation along the rotating shafts, misalignment between two or more shafts, asymmetry of the rotating shafts, wear between the rotor components, and the rub-impact force between the rotor and stator, etc. Accordingly, many research articles that discuss rotating machine vibration analysis and control are published and still published daily in order to find the best and optimal design for such machines to be safe in operation with low vibration levels. Yamamoto [1], Enrich [2], and Ganesan [3] discussed the influence of bearing clearance on the dynamical behaviors of both the symmetric and asymmetric rotating shaft systems, where they concluded that the rotor system may lose its stability at the primary resonance as a result of the bearing clearance. Yamamoto et al. [4-6] studied the nonlinear dynamics of the rotor system having cubic nonlinear spring characteristics at the primary, $\frac{1}{2}-$order, and $\frac{1}{3}-$order subharmonic resonance conditions. Chávez et al. [7] and Saeed [8] investigated the nonlinear oscillation of an asymmetric rotor system having both quadratic and cubic nonlinearity and excited with both external and parametric forces, simultaneously. Based on the acquired results, the authors reported that the system can perform either forward, backward, or both forward and backward motion depending on the asymmetric stiffness coefficients. In addition, the quasi-period and chaotic motions have been reported in the case of the nonlinear restoring force of the rotor system [9, 10]. Han and Chu [11], and Saeed et al. [12-14] investigated the nonlinear dynamical behaviors of a rotor system having transverse cracks. The authors concluded that the system may respond with strong vibration amplitudes due to the parametric excitations that arise as a result of the cracks breathing even if the shaft eccentricity is too small. Because nonlinearity is the inherent phenomenon in the rotating machinery, the small excitation sources cause a large vibration amplitude which may be larger than the air gap between the rotor and stator, which ultimately causes what is known as the rub-impact force between the rotor and the stator [15-21]. It is reported that the existence of the rub-impact force between the rotor and stator may result in one of three motions, which are period-n, quasi-periodic, or chaotic motion.

Although the vibration of the rotating machine is an undesired phenomenon, it is not avoidable using passive control techniques. The passive vibrations control technique depends on changing the dynamics of the targeted system

Manuscript received [23 March 2023]; revised [4 May 2023]; accepted [15 May 2023]. Date of publication [26 July 2023].

This work was supported by the National Science Centre, Poland under grant number OPUS 14 No. 2017/27/B/ST8/01330. (*Corresponding author: Nasser. A. Saeed).*

Osama M. Omara is with the Faculty of Electronic Engineering, Menoufia University, PO Box 32952, Menouf, Egypt (e-mail: osama.mohammed17@el-eng.menofia.edu.eg).

M. Sayed is with the Faculty of Electronic Engineering, Menoufia University, PO Box 32952, Menouf, Egypt (e-mail: mohamed.abdelkader @el-eng.menofia.edu.eg).

Nasser. A. Saeed is with the Faculty of Electronic Engineering, Menoufia University, PO Box 32952, Menouf, Egypt (e-mail: Nasser.AbdELhamid@el-eng.menofia.edu.eg).

This work is licensed under a Creative Commons Attribution 4.0 License. For more information, see https://creativecommons.org/licenses/by/4.0/

via coupling it with some kinds of absorbers that consist of mass, springs, and damper. On the other hand, Active control techniques depend on coupling the targeted oscillatory system to some kind of controller via both a network of sensors and actuators to mitigate the system's undesired vibrations. Passive control is not the preferred strategy with the rotating machinery because coupling an absorber consisting of mass, spring, and damper to mitigate the rotor's unwanted vibration is not an easy task. Therefore, different active control techniques have been presented to eliminate or at least suppress these vibrations to a satisfactory level. Eissa and Saeed [22] introduced a novel active control method to suppress the undesired vibrations of a nonlinear rotor system. The authors introduced two second-order fillers that are coupled to the rotor system linearly to act as active controllers. Ishida and Inoue [23] introduced a vibration absorber to suppress the lateral vibration of a vertically supported rotor using 4-pole electromagnets as an active absorber. The authors designed their controller based on the push-pull control force to mitigate the rotor vibration in both the horizontal and vertical directions. Saeed and Kamel [24], applied a $PD-$controller to mitigate the undesired oscillation of a nonlinear Jeffcott rotor system utilizing a 4-pole electromagnetic bearings system. The nonlinear vibration control and eliminating the rub-impact forces of the nonlinear rotor systems using different control techniques and 4-pole electromagnetic bearings actuator has been discussed [25-27]. In general, The electromagnetic bearings system is an active actuator that can be used easily to apply a controllable electromagnetic attractive force to control the rotors' lateral vibrations without any physical contact. Many configurations with different control techniques have been investigated [28-33]. Recently, Saeed et al. [34] studied the nonlinear vibration control of a vertically supported rotor system using a Proportional Integral Resonant Controller (PIR) and an $8-$pole actuator. The authors included the rub-impact force in the studied mathematical model. Based on the introduced analysis they reported that the rotor system may respond with one of three oscillation modes, which are no rub-impact, partial rub-impact, and full annular rub modes. In addition, it is concluded that the applied controller can reduce the system vibrations to a satisfactory level and prevent the rub-impact force between the rotor and its housing.

The current paper is intended to investigate the vibration control of a nonlinear rotor system governed by two coupled second-order differential equations and having both cubic and quadratic nonlinearities. A combination of both the $P-$controller and the integral resonant controller is employed to reduce the system's undesired oscillations. The proposed control technique is integrated into the system using an 8-pole electromagnetic bearings system as an actuator. The whole system mathematical model is derived and then analyzed analytically and numerically. The performance of the proposed controller in reducing the rotor's undesired vibrations is explored. Finally, the main results have been reported in the conclusions section.

In comparison with previously published work, however many control techniques have been applied to suppress the undesired vibration of the horizontally supported rotor system such as PD, PPF, and time-delayed controllers. It is the first time to apply the PIRC- controller to mitigate the lateral oscillation of the horizontally supported rotor system utilizing an 8-pole active magnetic bearing as an actuator. Based on the introduced analysis, the obtained results demonstrated the possibility of avoiding the rotor resonance frequency by changing the proportional controller gains. In addition, one can increase the system equivalent damping coefficients using the control gains of the integral resonant controller, which ultimately eliminates the nonlinear characteristics and forces the system to respond as a linear one.

II. Equations of Motion

The equations of motion that describe the lateral vibration of the considered system shown in Figure (1A) are given as follows [35]:

$$m\ddot{x}(\tau)+c\dot{x}(\tau)+F_X=me_d\omega^2\cos(\omega\tau) \tag{1}$$

$$m\ddot{y}(\tau)+c\dot{y}(\tau)+F_Y=me_d\omega^2\sin(\omega\tau)+mg \tag{2}$$

where m denotes the rotor mass in kilogram, c is the linear damping in $N.s/m$, F_{RX} and F_{RY} denote the restoring forces in N in X and Y directions, respectively, e_d is the disc eccentricity in meters, ω is the spinning speed in s^{-1}, and τ is the time in s. The rotor restoring force F_R has been modeled as a cubic nonlinear function of the radial displacement $R=\overline{OG}$ of the rotating shaft (see Figure (1B)), such that $F_R=k_LR+K_NR^3$ [35], where k_L and k_N are the linear and nonlinear stiffness coefficients, respectively. Accordingly, the horizontal and the vertical restoring forces F_X and F_Y in Equations (1) and (2) can be expressed as follows:

$$\begin{aligned}F_X&=\left[k_LR+k_NR^3\right]\cos(\theta)=\left[k_L+k_NR^2\right]R\cos(\theta)\\&=k_Lx(\tau)+k_N\left[x^3(\tau)+x(\tau)y^2(\tau)\right]\end{aligned} \tag{3}$$

$$\begin{aligned}F_Y&=\left[k_LR+k_NR^3\right]\sin(\theta)=\left[k_L+k_NR^2\right]R\sin(\theta)\\&=k_Ly(\tau)+k_N\left[y^3(\tau)+x^2(\tau)y(\tau)\right]\end{aligned} \tag{4}$$

Inserting Equations (4) and (5) into Equations (1) and (2), yields

$$\begin{aligned}&m\ddot{x}(\tau)+c\dot{x}(\tau)+k_Lx(\tau)+k_N\left(x^3(\tau)+x(\tau)y^2(\tau)\right)\\&=me_d\omega^2\cos(\omega\tau)\end{aligned} \tag{5}$$

$$\begin{aligned}&m\ddot{y}(\tau)+c\dot{y}(\tau)+k_Ly(\tau)+k_N\left(y^3(\tau)+x^2(\tau)y(\tau)\right)\\&=me_d\omega^2\sin(\omega\tau)+mg\end{aligned} \tag{6}$$

At the static equilibrium, we have $x=\dot{x}=\dot{y}=\ddot{x}=\ddot{y}=\omega=0$, and $y=y_{st}$, where y_{st} is the static displacement of the rotating disc below the $X-$axis due to both the disc and shaft weights as shown in Figure (1A). Substituting this condition) i.e., $x=\dot{x}=\dot{y}=\ddot{x}=\ddot{y}=\omega=0$, and $y=y_{st}$) into Equations (5) and (6), we have

$$k_Ly_{st}+k_Ny_{st}^3=mg \tag{7}$$

One can eliminate the constant mg from Equations (6) by introducing the new coordinate system X and Y such that $X = x$ and $Y = y - y_{st}$ into Equations (5) and (6), taking into account Equation (7) one can obtain the following modified equations of motion:

$$m\ddot{X} + c_1\dot{X} + (k_L + k_N y_{st}^2)X + 2k_N y_{st} XY + k_N(X^3 + XY^2) = me\omega^2 \cos(\omega\tau) \quad (8)$$

$$m\ddot{Y} + c_2\dot{Y} + (k_L + 3k_N y_{st}^2)Y + k_N y_{st}(X^2 + 3Y^2) + k_N(Y^3 + YX^2) = me\omega^2 \sin(\omega\tau) \quad (9)$$

The main purpose of this paper is to mitigate the nonlinear oscillation of the considered nonlinear system given by Equations (8) and (9). Accordingly, the eight-pole active magnetic bearing system has been introduced as an active actuator to apply control action on the rotor system in the form of magnetic attractive forces as shown in Figure (2). Therefore, Equations (8) and (9) can be modified after control to become:

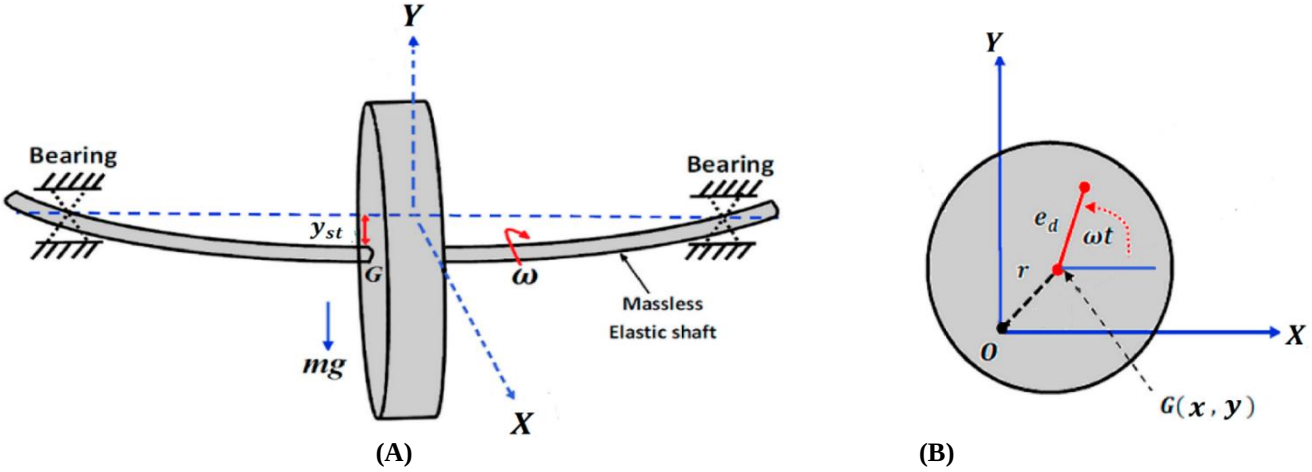

(A) **(B)**

Figure 1. Horizontally supported nonlinear rotor system: (A) system at static equilibrium, and (B) the rotating disc

$$m\ddot{X} + c_1\dot{X} + (k_L + k_N y_{st}^2)X + 2k_N y_{st} XY + k_N(X^3 + XY^2) = me\omega^2 \cos(\omega\tau) + F_{MX} \quad (10)$$

$$m\ddot{Y} + c_2\dot{Y} + (k_L + 3k_N y_{st}^2)Y + k_N y_{st}(X^2 + 3Y^2) + k_N(Y^3 + YX^2) = me\omega^2 \sin(\omega\tau) + F_{MY} \quad (11)$$

where F_{MX} and F_{MY} denote the control forces generated by the eight-pole actuator in X and Y directions, respectively. According to the eight-pole actuator shown in Figure (2), the control forces F_{MX} and F_{MY} can be obtained as follows:

$$F_{MX} = F_1 - F_5 + (F_2 + F_8 - F_4 - F_6)\cos(\beta) \quad (12)$$

$$F_{MY} = F_3 - F_7 + (F_2 + F_4 - F_6 - F_8)\cos(\beta) \quad (13)$$

where $F_1, F_2, \ldots, F_8$ are the eight forces generated by the eight-pole active magnetic bearing system

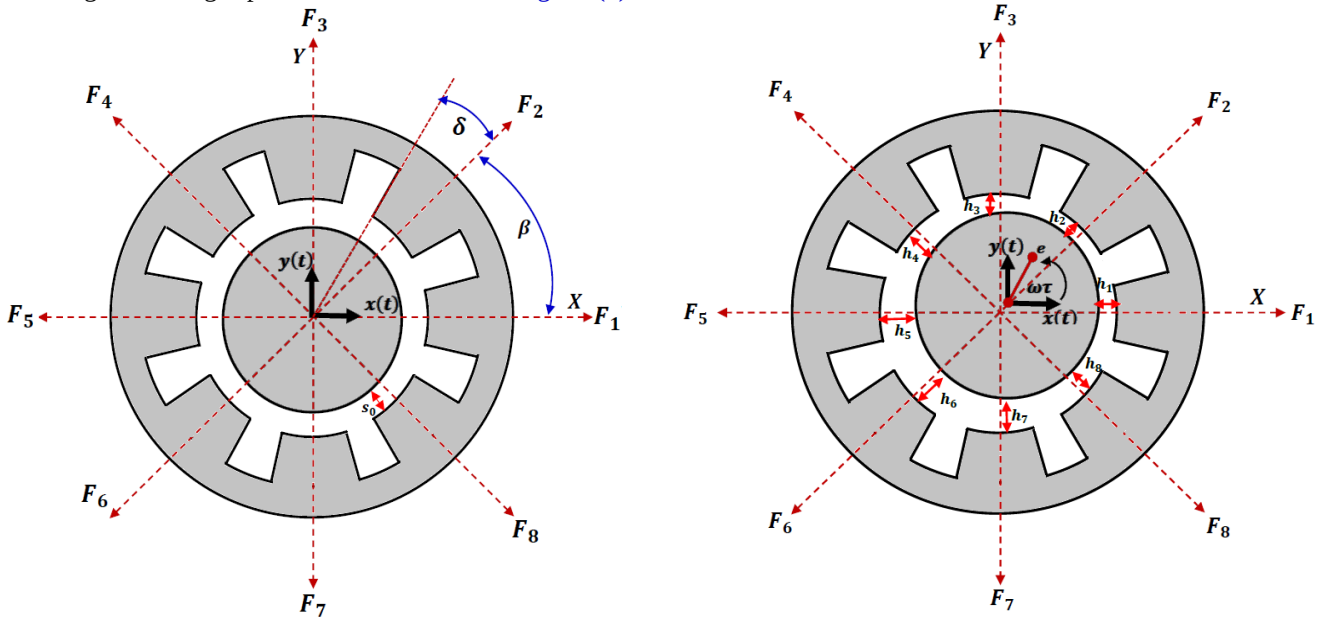

Figure 2. the rotor system coupled with 8-pole electromagnetic bearings

.

Based on the electromagnetic theory, the attractive electromagnetic force $F_j, \{j = 1,2,3,\dots,8\}$ can be expressed as follows [36]:

$$F_j = \frac{1}{4}\mu_0 N^2 A cos(\delta)\frac{I_j^2}{h_j^2} \tag{14}$$

where $\mu_0 N^2 A\cos(\delta)$ is constant, I_j is the electrical current of the j^{th} magnetic pole, and h_j is the air gap size between the rotating disc and the j^{th} magnetic pole. For the rotor displacements $X(\tau)$ and $Y(\tau)$, the air-gape size between the rotating disc and the j^{th} the magnetic pole can be expressed as follows:

$$\left.\begin{aligned}
h_1(X,Y) &= s_0 - X,\\
h_2(X,Y) &= s_0 - X\cos(\beta) - Y\cos(\beta),\\
h_3(X,Y) &= s_0 - Y,\\
h_4(X,Y) &= s_0 + X\cos(\beta) - Y\cos(\beta),\\
h_5(X,Y) &= s_0 + X,\\
h_6(X,Y) &= s_0 + X\cos(\beta) + Y\cos(\beta),\\
h_7(X,Y) &= s_0 + Y,\\
h_8(X,Y) &= s_0 - X\cos(\beta) + Y\cos(\beta).
\end{aligned}\right\} \tag{15}$$

where s_0 is the nominal air-gap size between each electromagnetic pole and the rotating disc, and $\beta = 45^o$. The electrical current I_j is designed to be a summation of two currents such that:

$$I_j = I_0 + i_j, \qquad j = 1,2,\dots,8 \tag{16}$$

where I_0 is a constant current for the pre-magnetization of the eight-pole system, and i_j is the control current of the j^{th} magnetic pole. Within this article, the introduced controller is designed to be a combination of both the $P-$ and $IRC-$controllers such that:

$$\left.\begin{aligned}
I_1 &= I_0 - k_1 X + k_2 U\\
I_2 &= I_0 - k_1 X\cos(\alpha) + k_2 U\cos(\alpha)\\
&\quad - k_3 Y\cos(\alpha) + k_4 V\cos(\alpha)\\
I_3 &= I_0 - k_3 Y + k_4 V\\
I_4 &= I_0 + k_1 X\cos(\alpha) - k_2 U\cos(\alpha)\\
&\quad - k_3 Y\cos(\alpha) + k_4 V\cos(\alpha)\\
I_5 &= I_0 + k_1 X - k_2 U\\
I_6 &= I_0 + k_1 X\cos(\alpha) - k_2 U\cos(\alpha)\\
&\quad + k_3 Y\cos(\alpha) - k_4 V\cos(\alpha)\\
I_7 &= I_0 + k_3 Y - k_4 V\\
I_8 &= I_0 - k_1 X\cos(\alpha) + k_2 U\cos(\alpha)\\
&\quad + k_3 Y\cos(\alpha) - k_4 V\cos(\alpha)
\end{aligned}\right\} \tag{17}$$

where k_1, k_3 are the control gains of the $P-$controller in X and Y directions, while k_2, k_4 are the control gains of the $IRC-$controller in X and Y directions. The equations of motion of the $IRC-$controllers are given such that [34]:

$$\dot{U} + \rho_1 U = \gamma_1 X, \tag{18}$$

$$\dot{V} + \rho_2 V = \gamma_2 Y. \tag{19}$$

where γ_1 and γ_2 are the feedback gains of the $IRC-$controller, while ρ_1 and ρ_2 are the internal feedback gains. Figure (3) show the block diagram that illustrates the interconnection between the rotor system and the proposed controller. Substituting Equations (12) to (17) into Equations (10), (11), (18), and (19), with introducing the dimensionless variables $q_1 = \frac{X}{s_0}$, $q_2 = \frac{Y}{s_0}$, $q_3 = \frac{U}{s_0}$, $q_4 = \frac{V}{s_0}$, $t = \omega_n\tau$, $y_{st} = 0.5s_0$, $\mu = \frac{c}{m\omega_n}$, $\delta_1 = \frac{s_0}{I_0}k_1$, $\delta_2 = \frac{s_0}{I_0}k_2$, $\delta_3 = \frac{s_0}{I_0}k_3$, $\delta_4 = \frac{s_0}{I_0}k_4$, $\lambda = \frac{k_N}{m\omega_n^2}$, $E = \frac{e}{s_0}$, $\Omega = \frac{\omega}{\omega_n}$, $\lambda_1 = \frac{\rho_1}{\omega_n}$, $\lambda_2 = \frac{\rho_2}{\omega_n}$, $\eta_1 = \frac{\gamma_1}{\omega_n}$, $\eta_2 = \frac{\gamma_2}{\omega_n}$, and $\omega_n = \sqrt{\frac{k_L}{m}} = \sqrt{\frac{\mu_0 I_0^2 N^2 Acos(\delta)}{4ms_0^3}}$ yields:

$$\begin{aligned}
&\ddot{q}_1 + \mu_1\dot{q}_1 + \omega_1^2 q_1 + \Delta_1 q_1 q_2 + \Delta_2(q_1^3 + q_1 q_2^2) =\\
&E\Omega^2\cos(\Omega t) + \rho_{10}q_1 + \rho_{11}q_3 + \rho_{12}q_1 q_2^2 + \rho_{13}q_1 q_3^2\\
&+\rho_{14}q_1 q_4^2 + \rho_{15}q_1^2 q_3 + \rho_{16}q_2^2 q_3 + \rho_{17}q_1 q_2 q_4\\
&+\rho_{18}q_2 q_3 q_4 + \rho_{19}q_1^3
\end{aligned} \tag{20}$$

$$\begin{aligned}
&\ddot{q}_2 + \mu_2\dot{q}_2 + \omega_2^2 q_2 + \frac{1}{2}\Delta_1(q_1^2 + 3q_2^2) + \Delta_2(q_2^3 + q_2 q_1^2) =\\
&E\Omega^2\sin(\Omega t) + \rho_{20}q_2 + \rho_{21}q_4 + \rho_{22}q_2 q_1^2 + \rho_{23}q_2 q_4^2\\
&+\rho_{24}q_2 q_3^2 + \rho_{25}q_2^2 q_4 + \rho_{26}q_1^2 q_4 + \rho_{27}q_1 q_2 q_3\\
&+\rho_{28}q_1 q_3 q_4 + \rho_{29}q_2^3
\end{aligned} \tag{21}$$

$$\dot{q}_3 + \lambda_1 q_3 = \eta_1 q_1 \tag{22}$$

$$\dot{q}_4 + \lambda_2 q_4 = \eta_2 q_2 \tag{23}$$

where

$$\begin{aligned}
\rho_{10} &= 4 + 8\cos^2(\alpha) - 8\delta_1\cos^2(\alpha) - 4\delta_1\\
\rho_{11} &= 8\delta_2\cos^2(\alpha) + 4\delta_2\\
\rho_{12} &= 8\delta_3^2\cos^4(\alpha) + 48\cos^4(\alpha) + 16\delta_1\delta_3\cos^4(\alpha)\\
&\quad -48\delta_3\cos^4(\alpha) - 24\delta_1\cos^4(\alpha)\\
\rho_{13} &= 8\delta_2^2\cos^4(\alpha) + 4\delta_2^2\\
\rho_{14} &= 8\delta_4^2\cos^4(\alpha)\\
\rho_{15} &= 12\delta_2 - 8\delta_1\delta_2 - 16\delta_1\delta_2\cos^4(\alpha) + 24\delta_2\cos^4(\alpha)\\
\rho_{16} &= 24\delta_2\cos^4(\alpha) - 16\delta_2\delta_3\cos^4(\alpha)\\
\rho_{17} &= 48\delta_4\cos^4(\alpha) - 16\delta_3\delta_4\cos^4(\alpha) - 16\delta_1\delta_4\cos^4(\alpha)\\
\rho_{18} &= 16\delta_2\delta_4\cos^4(\alpha)
\end{aligned}$$

$$\rho_{19} = 4\delta_1^2 + 8 - 24\delta_1\cos^4(\alpha) + 16\cos^4(\alpha) - 12\delta_1 + 8\delta_1^2\cos^4(\alpha)$$

$$\rho_{20} = 4 + 8\cos^2(\alpha) - 8\delta_3\cos^2(\alpha) - 4\delta_3$$

$$\rho_{21} = 8\delta_4\cos^2(\alpha) + 4\delta_4$$

$$\rho_{22} = 8\delta_1^2\cos^4(\alpha) + 48\cos^4(\alpha) + 16\delta_1\delta_3\cos^4(\alpha) - 48\delta_1\cos^4(\alpha) - 24\delta_3\cos^4(\alpha)$$

$$\rho_{23} = 8\delta_4^2\cos^4(\alpha) + 4\delta_4^2$$

$$\rho_{24} = 8\delta_2^2\cos^4(\alpha)$$

$$\rho_{25} = 12\delta_4 - 8\delta_3\delta_4 - 16\delta_3\delta_4\cos^4(\alpha) + 24\delta_4\cos^4(\alpha)$$

$$\rho_{26} = 24\delta_4\cos^4(\alpha) - 16\delta_1\delta_4\cos^4(\alpha)$$

$$\rho_{27} = 48\delta_2\cos^4(\alpha) - 16\delta_1\delta_2\cos^4(\alpha) - 16\delta_2\delta_3\cos^4(\alpha)$$

$$\rho_{28} = 16\delta_2\delta_4\cos^4(\alpha)$$

$$\rho_{29} = 4\delta_3^2 + 8 - 24\delta_3\cos^4(\alpha) + 16\cos^4(\alpha) - 12\delta_3 + 8\delta_3^2\cos^4(\alpha)$$

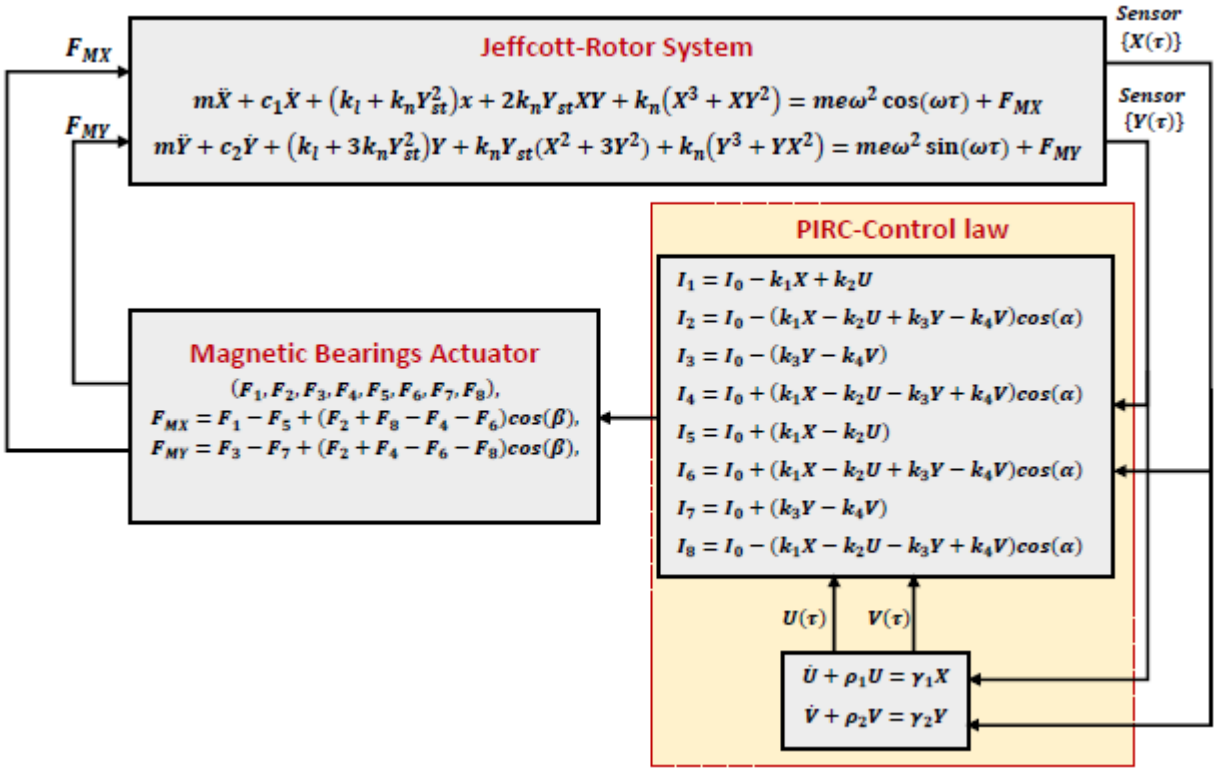

Figure 3. Block diagram to show the engineering implementation of the proposed control technique.

III. Analytical Solution

To investigate the nonlinear oscillations of the controlled system given by Equations (20) to (23), the multiple time scale perturbation technique has been applied with this section to find a second-order approximate solution of Equations (20) to (23) as follows [37, 40]:

$$q_1(t,\varepsilon) = q_{10}(T_0,T_1,T_2) + \varepsilon q_{11}(T_0,T_1,T_2) + \varepsilon^2 q_{12}(T_0,T_1,T_2) \quad (24)$$

$$q_2(t,\varepsilon) = q_{20}(T_0,T_1,T_2) + \varepsilon q_{21}(T_0,T_1,T_2) + \varepsilon^2 q_{22}(T_0,T_1,T_2) \quad (25)$$

$$q_3(t,\varepsilon) = \varepsilon q_{30}(T_0,T_1,T_2) + \varepsilon^2 q_{31}(T_0,T_1,T_2) \quad (26)$$

$$q_4(t,\varepsilon) = \varepsilon q_{40}(T_0,T_1,T_2) + \varepsilon^2 q_{41}(T_0,T_1,T_2) \quad (27)$$

where $T_j = \varepsilon^j t, \quad \{j = 0,1,2\}$. Using the chain rule of differentiation, one can express the ordinary derivatives $\frac{d}{dt}$ and $\frac{d^2}{dt^2}$ using partial differentiation rules as:

$$\left.\begin{aligned} \frac{d}{dt} &= D_0 + \varepsilon D_1 + \varepsilon^2 D_2, \\ \frac{d^2}{dt^2} &= D_0^2 + 2\varepsilon D_0 D_1 + \varepsilon^2(D_1^2 + 2D_2 D_0), \\ D_j &= \frac{\partial}{\partial T_j}, \quad j = 0,1,2 \end{aligned}\right\} \quad (28)$$

Following the perturbations procedure, the system parameters have been re-scaled such that:

$$\mu_1 = \varepsilon^2\tilde{\mu}_1, \mu_2 = \varepsilon^2\tilde{\mu}_2, \; E = \varepsilon^2\tilde{E}, \; \Delta_1 = \varepsilon\tilde{\Delta}_1, \; \Delta_2 = \varepsilon^2\tilde{\Delta}_2, \; \rho_{jk} = \varepsilon^2\tilde{\rho}_{jk}, \; j = 1,2, \quad k = 0,1 \quad (29)$$

Substituting Equations (24) to (29) into Equations (20) to (23), one can obtain the following set of solvable differential equations:

O (ε^0):

$$(D_0^2+\omega_1^2)q_{10}=0 \tag{30}$$

$$(D_0^2+\omega_2^2)q_{20}=0 \tag{31}$$

O (ε^1):

$$(D_0^2+\omega_1^2)q_{11}=-2D_0D_1q_{10}-\tilde{\Delta}_1q_{10}q_{20} \tag{32}$$

$$(D_0^2+\omega_2^2)q_{21}=-2D_0D_1q_{20}-\frac{1}{2}\tilde{\Delta}_1(q_{10}^2+3q_{20}^2) \tag{33}$$

O (ε^2):

$$\left(D_0+\lambda_1\right)q_{30}=\tilde{\eta}_1q_{10} \tag{34}$$

$$\left(D_0+\lambda_2\right)q_{40}=\tilde{\eta}_2q_{20} \tag{35}$$

$$\begin{aligned}(D_0^2+\omega_1^2)q_{12}=&-2D_0D_1q_{11}-\tilde{\mu}_1D_0q_{10}-\tilde{\Delta}_1q_{11}q_{20}\\&-\tilde{\Delta}_1q_{10}q_{21}-\tilde{\Delta}_2q_{10}^3-\tilde{\Delta}_2q_{10}q_{20}^2-D_1^2q_{10}\\&-2D_0D_2q_{10}+\tilde{\rho}_{10}q_{10}+\tilde{\rho}_{11}q_{30}\\&+\tilde{\rho}_{12}q_{10}q_{20}^2+\tilde{\rho}_{13}q_{10}q_{30}^2+\tilde{\rho}_{14}q_{10}q_{40}^2\\&+\tilde{\rho}_{15}q_{10}^2q_{30}+\tilde{\rho}_{16}q_{20}^2q_{30}+\tilde{\rho}_{17}q_{10}q_{20}q_{40}\\&+\tilde{\rho}_{18}q_{20}q_{30}q_{40}+\tilde{\rho}_{19}q_{10}^3+\tilde{E}\Omega^2\cos(\Omega T_0)\end{aligned} \tag{36}$$

$$\begin{aligned}(D_0^2+\omega_2^2)q_{22}=&-2D_0D_1q_{21}-\tilde{\mu}_2D_0q_{20}-\tilde{\Delta}_1q_{10}q_{11}\\&-3\tilde{\Delta}_1q_{20}q_{21}-\tilde{\Delta}_2q_{20}^3-\tilde{\Delta}_2q_{20}q_{10}^2\\&-2D_0D_2q_{20}-D_1^2q_{20}+\tilde{\rho}_{20}q_{20}+\tilde{\rho}_{21}q_{40}\\&+\tilde{\rho}_{22}q_{20}q_{10}^2+\tilde{\rho}_{23}q_{20}q_{40}^2+\tilde{\rho}_{24}q_{20}q_{30}^2\\&+\tilde{\rho}_{25}q_{20}^2q_{40}+\tilde{\rho}_{26}q_{10}^2q_{40}+\tilde{\rho}_{27}q_{10}q_{20}q_{30}\\&+\tilde{\rho}_{28}q_{10}q_{30}q_{40}+\tilde{\rho}_{29}q_{20}^3+\tilde{E}\Omega^2\sin(\Omega T_0)\end{aligned} \tag{37}$$

The solutions to Equations (٣٠), (٣١), (34), and (35) can be expressed as follows:

$$q_{10}(T_0,T_1,T_2)=A(T_1,T_2)e^{i\omega_1T_0}+\overline{A}(T_1,T_2)e^{-i\omega_1T_0}, \tag{38}$$

$$q_{20}(T_0,T_1,T_2)=B(T_1,T_2)e^{i\omega_2T_0}+\overline{B}(T_1,T_2)e^{-i\omega_2T_0}, \tag{39}$$

$$q_{30}(T_0,T_1,T_2)=\delta_1A(T_1,T_2)e^{i\omega_1T_0}+\overline{\delta}_1\overline{A}(T_1,T_2)e^{-i\omega_1T_0}, \tag{40}$$

$$q_{40}(T_0,T_1,T_2)=\delta_2B(T_1,T_2)e^{i\omega_2T_0}+\overline{\delta}_2\overline{B}(T_1,T_2)e^{-i\omega_2T_0} \tag{41}$$

where $i=\sqrt{-1}$, , $\delta_1=\frac{\lambda_1-i\omega_1}{\lambda_1^2+\omega_1^2}\tilde{\eta}_1, \delta_2=\frac{\lambda_2-i\omega_2}{\lambda_2^2+\omega_2^2}\tilde{\eta}_2$, while A and B are four unknown functions that will be defined in the following stages of analysis. Substituting Equations (38) and (39) into Equations (32) and (33), we have

$$\begin{aligned}q_{11}(T_0,T_1,T_2)=&\frac{AB\Delta_1}{\omega_2(2\omega_1+\omega_2)}e^{i(\omega_1+\omega_2)T_0}\\&+\frac{A\overline{B}\Delta_1}{\omega_2(\omega_2-2\omega_1)}e^{i(\omega_1-\omega_2)T_0}\end{aligned} \tag{42}$$

$$\begin{aligned}q_{21}(T_0,T_1,T_2)=&\frac{A^2\Delta_1}{2(4\omega_1^2-\omega_2^2)}e^{2iT_0\omega_1}+\frac{B^2\Delta_1}{2\omega_2^2}e^{2iT_0\omega_2}\\&-\frac{A\overline{A}\Delta_1}{\omega_2^2}-\frac{3B\overline{B}\Delta_1}{\omega_2^2}\end{aligned} \tag{43}$$

Now, inserting Equations (38) to (43) into Equations (36) and (37), yields

$$\begin{aligned}(D_0^2+\omega_1)q_{12}=&[\tilde{\rho}_{10}A+\tilde{\rho}_{11}\tilde{\delta}_1A+e^{2iT_0\sigma_2}\tilde{\rho}_{12}B^2\overline{A}\\&+2\tilde{\rho}_{12}AB\overline{B}+2\tilde{\rho}_{13}\tilde{\overline{\delta}}_1\tilde{\delta}_1A^2\overline{A}\\&+\tilde{\delta}_1^2\tilde{\rho}_{13}A^2\overline{A}+2\tilde{\delta}_2\tilde{\overline{\delta}}_2\tilde{\rho}_{14}AB\overline{B}\\&+e^{2iT_0\sigma_2}\tilde{\delta}_2^2\tilde{\rho}_{14}B^2\overline{A}+\tilde{\overline{\delta}}_1\tilde{\rho}_{15}A^2\overline{A}\\&+2\tilde{\delta}_1\tilde{\rho}_{15}A^2\overline{A}+e^{2iT_0\sigma_2}\tilde{\overline{\delta}}_1\tilde{\rho}_{16}B^2\overline{A}\\&+2\tilde{\delta}_1\tilde{\rho}_{16}AB\overline{B}+\tilde{\overline{\delta}}_2\rho_{17}AB\overline{B}\\&+\tilde{\delta}_2\tilde{\rho}_{17}AB\overline{B}+e^{2iT_0\sigma_2}\tilde{\delta}_2\tilde{\rho}_{17}B^2\overline{A}\\&+\tilde{\delta}_1\tilde{\overline{\delta}}_2\tilde{\rho}_{18}AB\overline{B}+\tilde{\delta}_1\tilde{\delta}_2\tilde{\rho}_{18}AB\overline{B}\\&+e^{2iT_0\sigma_2}\tilde{\overline{\delta}}_1\tilde{\delta}_2\tilde{\rho}_{18}B^2\overline{A}+3\tilde{\rho}_{19}A^2\overline{A}\\&-i\tilde{\mu}_1\omega_1A-3\tilde{\Delta}_2A^2\overline{A}-2\tilde{\Delta}_2AB\overline{B}\\&-\tilde{\Delta}_2e^{2iT_0\sigma_2}B^2\overline{A}+\frac{\tilde{\Delta}_1^2}{\omega_2^2}A^2\overline{A}\\&-\frac{e^{2iT_0\sigma_2}\tilde{\Delta}_1^2}{2\omega_2^2}B^2\overline{A}-\frac{\tilde{\Delta}_1^2}{8\omega_1^2-2\omega_2^2}A^2\overline{A}\\&+\frac{3\tilde{\Delta}_1^2}{\omega_2^2}AB\overline{B}-\frac{2\tilde{\Delta}_1^2}{-2\omega_1\omega_2+\omega_2^2}AB\overline{B}\\&-2i\omega_1D_1A]e^{i\omega_1T_0}+\frac{1}{2}\tilde{E}\Omega^2e^{i\varepsilon\tilde{\sigma}_1T_0}\\&+NST+cc\end{aligned} \tag{44}$$

$$
\begin{aligned}
(D_0^2+\omega_2)q_{22} = [&\tilde{\rho}_{20}B+\tilde{\rho}_{21}\tilde{\delta}_2 B+\tilde{\rho}_{22}e^{-2i\sigma_2 T_0}A^2\bar{B}\\
&+2\tilde{\rho}_{22}A\bar{A}B+2\tilde{\delta}_2\tilde{\bar{\delta}}_2\rho_{23}B^2\bar{B}\\
&+\tilde{\rho}_{23}\tilde{\delta}_2^2B^2\bar{B}+2\tilde{\rho}_{24}\tilde{\delta}_1\tilde{\bar{\delta}}_1A\bar{A}B\\
&+\rho_{24}\tilde{\delta}_1^2e^{-2i\sigma_2 T_0}A^2\bar{B}+\tilde{\bar{\delta}}_2\tilde{\rho}_{25}B^2\bar{B}\\
&+2\tilde{\delta}_2\tilde{\rho}_{25}B^2\bar{B}+\tilde{\bar{\delta}}_2\tilde{\rho}_{26}e^{-2i\sigma_2 T_0}A^2\bar{B}\\
&+2\tilde{\rho}_{26}\tilde{\delta}_2A\bar{A}B+\tilde{\rho}_{27}\tilde{\bar{\delta}}_1A\bar{A}B\\
&+\rho_{27}\tilde{\delta}_1A\bar{A}B+\tilde{\delta}_1\tilde{\rho}_{27}e^{-2i\sigma_2 T_0}A^2\bar{B}\\
&+\tilde{\delta}_1\tilde{\bar{\delta}}_2\rho_{28}e^{-2i\sigma_2 T_0}A^2\bar{B}+\tilde{\delta}_1\tilde{\delta}_2\tilde{\rho}_{28}A\bar{A}B\\
&+\tilde{\rho}_{28}\tilde{\bar{\delta}}_1\tilde{\delta}_2A\bar{A}B+3\tilde{\rho}_{29}B^2\bar{B}\\
&+\frac{9\tilde{\Delta}_1^2}{\omega_2^2}B^2\bar{B}-\frac{3e^{-2i\sigma_2 T_0}\tilde{\Delta}_1^2}{8\omega_1^2-2\omega_2^2}A^2\bar{B}\\
&-\frac{e^{-2i\sigma_2 T_0}\tilde{\Delta}_1^2}{-2\omega_1\omega_2+\omega_2^2}A^2\bar{B}+\frac{3\tilde{\Delta}_1^2}{\omega_2^2}A\bar{A}B\\
&-\frac{\tilde{\Delta}_1^2}{2\omega_1\omega_2+\omega_2^2}A\bar{A}B-2\tilde{\Delta}_2A\bar{A}B\\
&-\tilde{\Delta}_2e^{-2i\sigma_2 T_0}A^2\bar{B}-3\tilde{\Delta}_2B^2\bar{B}-i\tilde{\mu}_2\omega_2B\\
&-2i\omega_2D_1B\}e^{i\omega_2 T_0}-\frac{1}{2}i\tilde{E}\Omega^2e^{i\Omega T_0}\\
&+NST+cc
\end{aligned}
\tag{45}
$$

where cc denotes the complex conjugates terms, and NST stands for the non-secular term. To get a bounded solution for Equations (44) and (45), the coefficients of $e^{-i\omega_1 T_0}$ and $e^{-i\omega_2 T_0}$ should be vanished. So, the solvability conditions of Equations (44) and (45) at the primary resonance with 1:1 internal resonance condition (i.e., when $\Omega=\omega_1=\omega_2$), let the parameters σ_1 and σ_2 describe the closeness of Ω to ω_1 and ω_2 such that:

$$
\left.\begin{aligned}
\Omega &= \omega_1+\sigma_1=\omega_1+\varepsilon\hat{\sigma}_1,\\
\omega_2 &= \omega_1+\sigma_2=\omega_2+\varepsilon\hat{\sigma}_2
\end{aligned}\right\}
\tag{46}
$$

Inserting Equation (46) into Equations (44) and (45), we have

$$
\begin{aligned}
&-2i\omega_1D_1A+\tilde{\rho}_{10}A+\tilde{\rho}_{11}\tilde{\delta}_1A+\tilde{\rho}_{12}B^2\bar{A}e^{2iT_0\sigma_2}+2\tilde{\rho}_{12}AB\bar{B}\\
&+2\tilde{\rho}_{13}\tilde{\bar{\delta}}_1\tilde{\delta}_1A^2\bar{A}+\tilde{\delta}_1^2\tilde{\rho}_{13}A^2\bar{A}+2\tilde{\delta}_2\tilde{\bar{\delta}}_2\tilde{\rho}_{14}AB\bar{B}\\
&+\tilde{\delta}_2^2\tilde{\rho}_{14}B^2\bar{A}e^{2iT_0\sigma_2}+\tilde{\bar{\delta}}_1\tilde{\rho}_{15}A^2\bar{A}+2\tilde{\delta}_1\tilde{\rho}_{15}A^2\bar{A}\\
&+\tilde{\bar{\delta}}_1\tilde{\rho}_{16}B^2\bar{A}e^{2iT_0\sigma_2}+2\tilde{\delta}_1\tilde{\rho}_{16}AB\bar{B}+\tilde{\bar{\delta}}_2\rho_{17}AB\bar{B}\\
&+\tilde{\delta}_2\tilde{\rho}_{17}AB\bar{B}+\tilde{\delta}_2\tilde{\rho}_{17}B^2\bar{A}e^{2iT_0\sigma_2}+\tilde{\delta}_1\tilde{\bar{\delta}}_2\tilde{\rho}_{18}AB\bar{B}\\
&+\tilde{\delta}_1\tilde{\delta}_2\tilde{\rho}_{18}AB\bar{B}+\tilde{\bar{\delta}}_1\tilde{\delta}_2\tilde{\rho}_{18}B^2\bar{A}e^{2iT_0\sigma_2}+3\tilde{\rho}_{19}A^2\bar{A}\\
&-i\tilde{\mu}_1\omega_1A-3\tilde{\Delta}_2A^2\bar{A}-2\tilde{\Delta}_2AB\bar{B}-\tilde{\Delta}_2B^2\bar{A}e^{2iT_0\sigma_2}\\
&+\frac{\tilde{\Delta}_1^2}{\omega_2^2}A^2\bar{A}-\frac{\tilde{\Delta}_1^2}{2\omega_2^2}B^2\bar{A}e^{2iT_0\sigma_2}-\frac{\tilde{\Delta}_1^2}{8\omega_1^2-2\omega_2^2}A^2\bar{A}\\
&+\frac{3\tilde{\Delta}_1^2}{\omega_2^2}AB\bar{B}-\frac{2\tilde{\Delta}_1^2}{-2\omega_1\omega_2+\omega_2^2}AB\bar{B}+\frac{1}{2}\tilde{E}\Omega^2e^{i\sigma_1T_0}=0
\end{aligned}
\tag{47}
$$

$$
\begin{aligned}
&-2i\omega_2D_1B+\tilde{\rho}_{20}B+\tilde{\rho}_{21}\tilde{\delta}_2B+\tilde{\rho}_{22}A^2\bar{B}e^{-2i\sigma_2T_0}\\
&+2\tilde{\rho}_{22}A\bar{A}B+2\tilde{\delta}_2\tilde{\bar{\delta}}_2\rho_{23}B^2\bar{B}+\tilde{\rho}_{23}\tilde{\delta}_2^2B^2\bar{B}\\
&+2\tilde{\rho}_{24}\tilde{\delta}_1\tilde{\bar{\delta}}_1A\bar{A}B+\rho_{24}\tilde{\delta}_1^2A^2\bar{B}e^{-2i\sigma_2T_0}+\tilde{\bar{\delta}}_2\tilde{\rho}_{25}B^2\bar{B}\\
&+2\tilde{\delta}_2\tilde{\rho}_{25}B^2\bar{B}+\tilde{\bar{\delta}}_2\tilde{\rho}_{26}A^2\bar{B}e^{-2i\sigma_2T_0}+2\tilde{\rho}_{26}\tilde{\delta}_2A\bar{A}B\\
&+\tilde{\rho}_{27}\tilde{\bar{\delta}}_1A\bar{A}B+\rho_{27}\tilde{\delta}_1A\bar{A}B+\tilde{\delta}_1\tilde{\rho}_{27}A^2\bar{B}e^{-2i\sigma_2T_0}\\
&+\tilde{\delta}_1\tilde{\bar{\delta}}_2\rho_{28}A^2\bar{B}e^{-2i\sigma_2T_0}+\tilde{\delta}_1\tilde{\delta}_2\tilde{\rho}_{28}A\bar{A}B\\
&+\tilde{\rho}_{28}\tilde{\bar{\delta}}_1\tilde{\delta}_2A\bar{A}B+3\tilde{\rho}_{29}B^2\bar{B}+\frac{9\tilde{\Delta}_1^2}{\omega_2^2}B^2\bar{B}\\
&-\frac{3\tilde{\Delta}_1^2}{8\omega_1^2-2\omega_2^2}A^2\bar{B}e^{-2i\sigma_2T_0}-\frac{\tilde{\Delta}_1^2}{-2\omega_1\omega_2+\omega_2^2}A^2\bar{B}e^{-2i\sigma_2T_0}\\
&+\frac{3\tilde{\Delta}_1^2}{\omega_2^2}A\bar{A}B-\frac{\tilde{\Delta}_1^2}{2\omega_1\omega_2+\omega_2^2}A\bar{A}B-2\tilde{\Delta}_2A\bar{A}B\\
&-\tilde{\Delta}_2A^2\bar{B}e^{-2i\sigma_2T_0}-3\tilde{\Delta}_2B^2\bar{B}-i\tilde{\mu}_2\omega_2B-\frac{1}{2}i\tilde{E}\Omega^2e^{i\sigma_1T_0}=0
\end{aligned}
\tag{48}
$$

To analyze Equations (47) and (4^), the functions A and B can be expressed in the polar form such that $A=\frac{1}{2}ae^{i\theta_1}$ and $B=\frac{1}{2}be^{i\theta_2}$. Substituting these forms (i.e., $A=\frac{1}{2}ae^{i\theta_1}$ and $B=\frac{1}{2}be^{i\theta_2}$) into Equations (47) and (48), one can obtain the following autonomous system:

$$\dot{a} = -\frac{1}{2}\mu_1 a - \frac{\Delta_2 \sin(2\varphi_1 - 2\varphi_2)}{8\omega_1} ab^2 + \frac{\rho_{12}\sin(2\varphi_1 - 2\varphi_2)}{8\omega_1} ab^2 - \frac{1}{4}\frac{\eta_1^2\lambda_1\rho_{13}}{(\lambda_1^2+\omega_1^2)^2} a^3 - \frac{1}{2}\frac{\eta_1\rho_{11}}{(\lambda_1^2+\omega_1^2)} a - \frac{1}{8}\frac{\eta_1\rho_{15}}{(\lambda_1^2+\omega_1^2)} a^3 - \frac{1}{4}\frac{\eta_1\rho_{16}}{(\lambda_1^2+\omega_1^2)} ab^2 + \frac{\eta_1\rho_{16}\cos(2\varphi_1 - 2\varphi_2)}{8(\lambda_1^2+\omega_1^2)} ab^2 + \frac{\eta_1\lambda_1\rho_{16}\sin(2\varphi_1 - 2\varphi_2)}{8\omega_1(\lambda_1^2+\omega_1^2)} ab^2 - \frac{\Delta_1^2\sin(2\varphi_1 - 2\varphi_2)}{16\omega_1\omega_2^2} ab^2 + \frac{\eta_2^2\lambda_2^2\rho_{14}\sin(2\varphi_1 - 2\varphi_2)}{8\omega_1(\lambda_2^2+\omega_2^2)^2} ab^2 - \frac{\eta_2^2\rho_{14}\sin(2\varphi_1 - 2\varphi_2)}{8\omega_1(\lambda_2^2+\omega_2^2)^2} ab^2 - \frac{\eta_2^2\lambda_2\rho_{14}\cos(2\varphi_1 - 2\varphi_2)}{4\omega_1(\lambda_2^2+\omega_2^2)^2} ab^2 - \frac{1}{4}\frac{\eta_1\eta_2\lambda_2\rho_{18}}{(\lambda_1^2+\omega_1^2)(\lambda_1^2+\omega_2^2)} ab^2 + \frac{\eta_1\eta_2\lambda_2\rho_{18}\cos(2\varphi_1 - 2\varphi_2)}{8(\lambda_1^2+\omega_1^2)(\lambda_2^2+\omega_2^2)} ab^2 + \frac{\eta_1\eta_2\lambda_1\lambda_2\rho_{18}\sin(2\varphi_1 - 2\varphi_2)}{8\omega_1(\lambda_1^2+\omega_1^2)(\lambda_2^2+\omega_2^2)} - \frac{\eta_2\rho_{17}\cos(2\varphi_1 - 2\varphi_2)}{8\omega_1(\lambda_2^2+\omega_2^2)} ab^2 + \frac{\eta_1\eta_2\rho_{18}\omega_2\sin(2\varphi_1 - 2\varphi_2)}{8(\lambda_1^2+\omega_1^2)(\lambda_2^2+\omega_2^2)} ab^2 - \frac{\eta_1\eta_2\lambda_1\rho_{18}\omega_2\sin(2\varphi_1 - 2\varphi_2)}{8\omega_1(\lambda_1^2+\omega_1^2)(\lambda_2^2+\omega_2^2)} ab^2 + \frac{E\Omega^2}{2\omega_1}\sin(\varphi_1) \tag{49}$$

$$\dot{b} = -\frac{1}{2}\mu_2 b + \frac{\Delta_2\sin(2\varphi_1 - 2\varphi_2)}{8\omega_2} a^2 b - \frac{\eta_2\rho_{21}}{2(\lambda_2^2+\omega_2^2)} b - \frac{\rho_{22}\sin(2\varphi_1 - 2\varphi_2)}{8\omega_2} a^2 b - \frac{\eta_2^2\lambda_2\rho_{23}}{4(\lambda_2^2+\omega_2^2)^2} b^3 + \frac{\eta_1^2\rho_{24}\omega_1^2\sin(2\varphi_1 - 2\varphi_2)}{8\omega_2(\lambda_1^2+\omega_1^2)^2} a^2 b - \frac{\eta_1^2\lambda_1\rho_{24}\omega_1\cos(2\varphi_1 - 2\varphi_2)}{4\omega_2(\lambda_1^2+\omega_1^2)^2} a^2 b - \frac{\eta_1^2\lambda_1^2\rho_{24}\sin(2\varphi_1 - 2\varphi_2)}{8\omega_2(\lambda_1^2+\omega_1^2)^2} a^2 b - \frac{\eta_2\rho_{25}}{8(\lambda_2^2+\omega_2^2)} b^3 - \frac{\eta_2\rho_{26}}{4(\lambda_2^2+\omega_2^2)} a^2 b + \frac{\eta_2\rho_{26}\cos(2\varphi_1 - 2\varphi_2)}{8(\lambda_2^2+\omega_2^2)} a^2 b - \frac{\eta_2\lambda_2\rho_{26}\sin(2\varphi_1 - 2\varphi_2)}{8\omega_2(\lambda_2^2+\omega_2^2)} a^2 b - \frac{\eta_1\rho_{27}\omega_1\cos(2\varphi_1 - 2\varphi_2)}{8\omega_2(\lambda_1^2+\omega_1^2)} a^2 b - \frac{\eta_1\lambda_1\rho_{27}\sin(2\varphi_1 - 2\varphi_2)}{8(\lambda_1^2+\omega_1^2)} a^2 b - \frac{\eta_1\eta_2\rho_{28}\omega_1\sin(2\varphi_1 - 2\varphi_2)}{8(\lambda_1^2+\omega_1^2)(\lambda_2^2+\omega_2^2)} a^2 b - \frac{\eta_1\eta_2\lambda_1\rho_{28}}{4(\lambda_1^2+\omega_1^2)(\lambda_2^2+\omega_2^2)} a^2 b + \frac{\eta_1\eta_2\lambda_1\rho_{28}\cos(2\varphi_1 - 2\varphi_2)}{8(\lambda_1^2+\omega_1^2)(\lambda_2^2+\omega_2^2)} a^2 b - \frac{\eta_1\eta_2\lambda_2\rho_{28}\omega_1\cos(2\varphi_1 - 2\varphi_2)}{8(\lambda_1^2+\omega_1^2)(\lambda_2^2+\omega_2^2)} a^2 b - \frac{\eta_1\eta_2\lambda_1\lambda_2\rho_{28}\sin(2\varphi_1 - 2\varphi_2)}{8\omega_2(\lambda_1^2+\omega_1^2)(\lambda_2^2+\omega_2^2)} a^2 b + \frac{3\Delta_1^2\sin(2\varphi_1 - 2\varphi_2)}{8\omega_2(8\omega_1^2 - 2\omega_2^2)} a^2 b + \frac{\Delta_1^2\sin(2\varphi_1 - 2\varphi_2)}{8\omega_2(\omega_2^2 - 2\omega_1\omega_2)} a^2 b - \frac{1}{2\omega_2} E\Omega^2\cos(\varphi_2) \tag{50}$$

$$
\begin{aligned}
\dot{\varphi}_1 = {} & \sigma_1 - \frac{3\Delta_2}{8\omega_1}a^2 - \frac{\Delta_2}{4\omega_1}b^2 \\
& - \frac{\Delta_2\cos(2\varphi_1 - 2\varphi_2)}{8\omega_1}b^2 + \frac{\rho_{10}}{2\omega_1} \\
& + \frac{\eta_1\lambda_1\rho_{11}}{2\omega_1(\lambda_1^2+\omega_1^2)} + \frac{\rho_{12}}{4\omega_1}b^2 \\
& + \frac{\rho_{12}\cos(2\varphi_1 - 2\varphi_2)}{8\omega_1}b^2 + \frac{\eta_1^2\rho_{13}\omega_1}{8(\lambda_1^2+\omega_1^2)^2}a^2 \\
& + \frac{3\eta_1^2\lambda_1^2\rho_{13}}{8\omega_1(\lambda_1^2+\omega_1^2)^2}a^2 + \frac{\eta_2^2\rho_{14}}{4\omega_1(\lambda_2^2+\omega_2^2)^2}b^2 \\
& - \frac{\eta_2^2\rho_{14}\cos(2\varphi_1 - 2\varphi_2)}{8\omega_1(\lambda_2^2+\omega_2^2)^2}b^2 \\
& + \frac{\eta_2^2\rho_{14}\lambda_2\omega_2\sin(2\varphi_1 - 2\varphi_2)}{4\omega_1(\lambda_2^2+\omega_2^2)^2}b^2 \\
& + \frac{\eta_2^2\rho_{14}\lambda_2^2\omega_2^2}{4\omega_1(\lambda_2^2+\omega_2^2)^2}b^2 \\
& + \frac{\eta_2^2\lambda_2^2\rho_{14}\cos(2\varphi_1 - 2\varphi_2)}{8\omega_1(\lambda_2^2+\omega_2^2)^2}b^2 \\
& + \frac{3\eta_1\lambda_1\rho_{15}}{8\omega_1(\lambda_1^2+\omega_1^2)}a^2 \\
& - \frac{\eta_1\rho_{16}\sin(2\varphi_1 - 2\varphi_2)}{8(\lambda_1^2+\omega_1^2)}b^2 + \frac{\eta_1\lambda_1\rho_{16}}{4\omega_1(\lambda_1^2+\omega_1^2)}b^2 \\
& + \frac{\eta_1\lambda_1\rho_{16}\cos(2\varphi_1 - 2\varphi_2)}{8\omega_1(\lambda_1^2+\omega_1^2)}b^2 \\
& + \frac{\eta_2\rho_{17}\omega_2\sin(2\varphi_1 - 2\varphi_2)}{8\omega_1(\lambda_2^2+\omega_2^2)}b^2 + \frac{\eta_2\lambda_2\rho_{17}}{4\omega_1(\lambda_2^2+\omega_2^2)}b^2 \\
& + \frac{\eta_2\lambda_2\rho_{17}\cos(2\varphi_1 - 2\varphi_2)}{8\omega_1(\lambda_2^2+\omega_2^2)}b^2 \\
& + \frac{\eta_1\eta_2\rho_{18}\omega_2\cos(2\varphi_1 - 2\varphi_2)}{8(\lambda_1^2+\omega_1^2)(\lambda_2^2+\omega_2^2)}b^2 \\
& + \frac{\eta_1\eta_2\lambda_1\rho_{18}\omega_2\sin(2\varphi_1 - 2\varphi_2)}{8\omega_1(\lambda_1^2+\omega_1^2)(\lambda_2^2+\omega_2^2)}b^2 \\
& - \frac{\eta_1\eta_2\lambda_2\rho_{18}\sin(2\varphi_1 - 2\varphi_2)}{8\omega_1(\lambda_1^2+\omega_1^2)(\lambda_2^2+\omega_2^2)}b^2 \\
& + \frac{\eta_1\eta_2\lambda_1\lambda_2\rho_{18}}{4\omega_1(\lambda_1^2+\omega_1^2)(\lambda_2^2+\omega_2^2)}b^2 \\
& + \frac{\eta_1\eta_2\lambda_1\lambda_2\rho_{18}\cos(2\varphi_1 - 2\varphi_2)}{8\omega_1(\lambda_1^2+\omega_1^2)(\lambda_2^2+\omega_2^2)}b^2 + \frac{3\rho_{19}}{8\omega_1}a^2 \\
& + \frac{\Delta_1^2}{8\omega_1\omega_2^2}a^2 + \frac{3\Delta_1^2}{8\omega_1\omega_2^2}b^2 - \frac{\Delta_1^2\cos(2\varphi_1 - 2\varphi_2)}{16\omega_1\omega_2^2}b^2 \\
& - \frac{\Delta_1^2}{8\omega_1(8\omega_1^2 - 2\omega_2^2)}a^2 - \frac{\Delta_1^2}{8\omega_1(-2\omega_1\omega_2 + \omega_2^2)}b^2 \\
& - \frac{\Delta_1^2}{8\omega_1(2\omega_1\omega_2 + \omega_2^2)}b^2 + \frac{1}{2\omega_1 a}E\Omega^2\cos(\varphi_1)
\end{aligned}
\tag{51}
$$

$$
\begin{aligned}
\dot{\varphi}_2 = {} & \sigma_1 - \sigma_2 + \frac{3\Delta_1^2}{8\omega_2^3}a^2 + \frac{15\Delta_1^2}{16\omega_2^3}b^2 \\
& - \frac{3\Delta_1^2\cos(2\varphi_1 - 2\varphi_2)}{8\omega_2(8\omega_1^2 - 2\omega_2^2)}a^2 - \frac{\Delta_1^2\cos(2\varphi_1 - 2\varphi_2)}{8\omega_2(\omega_2^2 - 2\omega_1\omega_2)}a^2 \\
& - \frac{\Delta_1^2}{8\omega_2(\omega_2^2 + 2\omega_1\omega_2)}a^2 - \frac{\Delta_2}{4\omega_2}a^2 - \frac{3\Delta_2}{8\omega_2}b^2 \\
& - \frac{\Delta_2\cos(2\varphi_1 - 2\varphi_2)}{8\omega_2}a^2 + \frac{\rho_{20}}{2\omega_2} \\
& + \frac{\eta_2\lambda_2\rho_{21}}{2(\lambda_2^2+\omega_2^2)\omega_2} + \frac{\rho_{22}}{4\omega_2}a^2 \\
& + \frac{\rho_{22}\cos(2\varphi_1 - 2\varphi_2)}{8\omega_2}a^2 + \frac{\eta_2^2\rho_{23}}{8(\lambda_2^2+\omega_2^2)^2\omega_2}b^2 \\
& + \frac{3\lambda_2^2\eta_2^2\rho_{23}}{8(\lambda_2^2+\omega_2^2)^2\omega_2}b^2 + \frac{\eta_1^2\rho_{24}}{4(\lambda_1^2+\omega_1^2)^2\omega_2}a^2 \\
& - \frac{\rho_{24}\eta_1^2\cos(2\varphi_1 - 2\varphi_2)}{8(\lambda_1^2+\omega_1^2)^2\omega_2}a^2 \\
& - \frac{\rho_{24}\eta_1^2\lambda_1\sin(2\varphi_1 - 2\varphi_2)}{4(\lambda_1^2+\omega_1^2)^2\omega_2}a^2 \\
& + \frac{\rho_{24}\eta_1^2\lambda_1^2}{4(\lambda_1^2+\omega_1^2)^2\omega_2}a^2 \\
& + \frac{\rho_{24}\eta_1^2\lambda_1^2\cos(2\varphi_1 - 2\varphi_2)}{8(\lambda_1^2+\omega_1^2)^2\omega_2}a^2 + \frac{3\rho_{25}\eta_2\lambda_2}{8(\lambda_2^2+\omega_2^2)^2\omega_2}b^2 \\
& + \frac{\rho_{26}\eta_2\sin(2\varphi_1 - 2\varphi_2)}{8(\lambda_2^2+\omega_2^2)^2\omega_2}a^2 + \frac{\rho_{26}\eta_2\lambda_2}{4(\lambda_2^2+\omega_2^2)\omega_2}a^2 \\
& + \frac{\rho_{26}\eta_2\lambda_2\cos(2\varphi_1 - 2\varphi_2)}{8(\lambda_2^2+\omega_2^2)\omega_2}a^2 \\
& - \frac{\rho_{27}\eta_1\sin(2\varphi_1 - 2\varphi_2)}{8(\lambda_1^2+\omega_1^2)\omega_2}a^2 \\
& + \frac{\rho_{27}\eta_1\lambda_1}{4(\lambda_1^2+\omega_1^2)\omega_2}a^2 + \frac{\rho_{27}\eta_1\lambda_1\cos(2\varphi_1 - 2\varphi_2)}{8(\lambda_1^2+\omega_1^2)\omega_2}a^2 \\
& + \frac{\rho_{28}\eta_1\eta_2\cos(2\varphi_1 - 2\varphi_2)}{8(\lambda_1^2+\omega_1^2)(\lambda_2^2+\omega_2^2)\omega_2}a^2 \\
& + \frac{\rho_{28}\eta_1\eta_2\lambda_1\sin(2\varphi_1 - 2\varphi_2)}{8(\lambda_1^2+\omega_1^2)(\lambda_2^2+\omega_2^2)\omega_2}a^2 \\
& - \frac{\rho_{28}\eta_1\eta_2\lambda_2\sin(2\varphi_1 - 2\varphi_2)}{8(\lambda_1^2+\omega_1^2)(\lambda_2^2+\omega_2^2)\omega_2}a^2 \\
& + \frac{\rho_{28}\eta_1\eta_2\lambda_1\lambda_2}{4(\lambda_1^2+\omega_1^2)(\lambda_2^2+\omega_2^2)\omega_2}a^2 \\
& + \frac{\rho_{28}\eta_1\eta_2\lambda_1\lambda_2\cos(2\varphi_1 - 2\varphi_2)}{8(\lambda_1^2+\omega_1^2)(\lambda_2^2+\omega_2^2)\omega_2}a^2 + \frac{3\rho_{29}}{8\omega_2}b^2 \\
& + \frac{1}{2\omega_2 b}E\Omega^2\sin(\varphi_2)
\end{aligned}
\tag{52}
$$

where $a(t)$ and $b(t)$ are the oscillation amplitudes of the controlled system given by Equations (20)-(23) in the

horizontal and vertical direction, respectively, while $\varphi_1(t)$ and $\varphi_2(t)$ represent the motion phase angles in the horizontal and vertical directions, respectively. Accordingly, to investigate the steady-state vibration amplitudes of the system (20)-(23) as a function of the different parameters, one can solve the nonlinear algebraic system given by Equations (49)-(52) when setting $\dot{a} = \dot{b} = \dot{\varphi}_1 = \dot{\varphi}_2 = 0.0$.

IV. System Steady-State Dynamics

Within this section, the system steady-state vibration amplitudes (i.e., a, b) in both the horizontal and vertical directions have been explored before and after control. In addition, the influence of the different control parameters on the system dynamics has been investigated by solving Equations (49)-(52) when $\dot{a} = \dot{b} = \dot{\varphi}_1 = \dot{\varphi}_2 = 0.0$ utilizing one of the system parameters as a bifurcation parameter. Before proceeding further, it is important to mention that the coefficients $\delta_1 = \frac{s_0}{I_0} k_1$ and $\delta_3 = \frac{s_0}{I_0} k_3$ represent the dimensionless control gains of the proportional controller, while $\delta_2 = \frac{s_0}{I_0} k_2$ and $\delta_4 = \frac{s_0}{I_0} k_4$ denote the dimensionless control gains of the $IRC-$ controller. Accordingly, the performance of the proposed control technique can be explored via investigating the influence of both the control gains (i.e., $\delta_1, \delta_2, \delta_3, \delta_4$) on the steady-state vibration amplitudes (i.e., a and b) of the controlled system given by Equations (20)-(23). By solving Equations (49)-(52) when $\dot{a} = \dot{b} = \dot{\varphi}_1 = \dot{\varphi}_2 = 0.0$, one can obtain the different frequency response curves as given in Figures (4)-(8).

In Figure (4), the steady-state vibration amplitudes of the system have been plotted against the parameter σ_1 at different levels of the excitation amplitude E before control (i.e., when $\delta_1 = \delta_2 = \delta_3 = \delta_4 = 0$). The figure demonstrates that the lateral vibration in both the horizontal and vertical directions is a monotonic increasing function of E. In addition, the nonlinear characteristics dominate the rotor motion at the large magnitudes of the excitation amplitude E, where the system may respond with a multistable solution as well as exhibit jump phenomena if it is excited periodically with a frequency close to the system's natural frequency.

Accordingly, the main subject of this article is to mitigate the undesired high oscillation amplitudes (a and b) shown in Figure (4) to a small acceptable level as well as to eliminate the nonlinear behaviors of the rotor and force it to respond as a linear system regardless of the level of the excitation force using a proportional controller (i.e., δ_1 and δ_3) and integral resonant controller (i.e., δ_2 and δ_4), simultaneously. The effect of the proportional controller gains (i.e., when $\delta_1 = \delta_3 = 0.99,\ 1.0,$ and 1.01) on the system steady-state vibration amplitudes of the considered rotor system are illustrated in Figure (5). It is clear from the figure the small change of $\delta_1 = \delta_3$ has a great influence on the system's steady-state dynamics, where one can shift the system frequency response curve to the right (i.e., when setting $\delta_1 = \delta_3 = 1.01$) or to the left (i.e., when setting $\delta_1 = \delta_3 = 0.99$) in order to avoid the resonance frequency at $\sigma_1 \cong 0$.

In addition, the system dynamics at the different values of the integral resonant controller gains (i.e., when $\delta_2 = \delta_4 = 0.001, 0.005,$ and 0.01) has been illustrated in Figure (6). By examining Figure (6), one can deduce that the increase in the controller gains $\delta_2 = \delta_4$, decreases the oscillation amplitudes (a and b), and forces the system to respond as a linear system via increasing the equivalent damping coefficients if the rotor system.

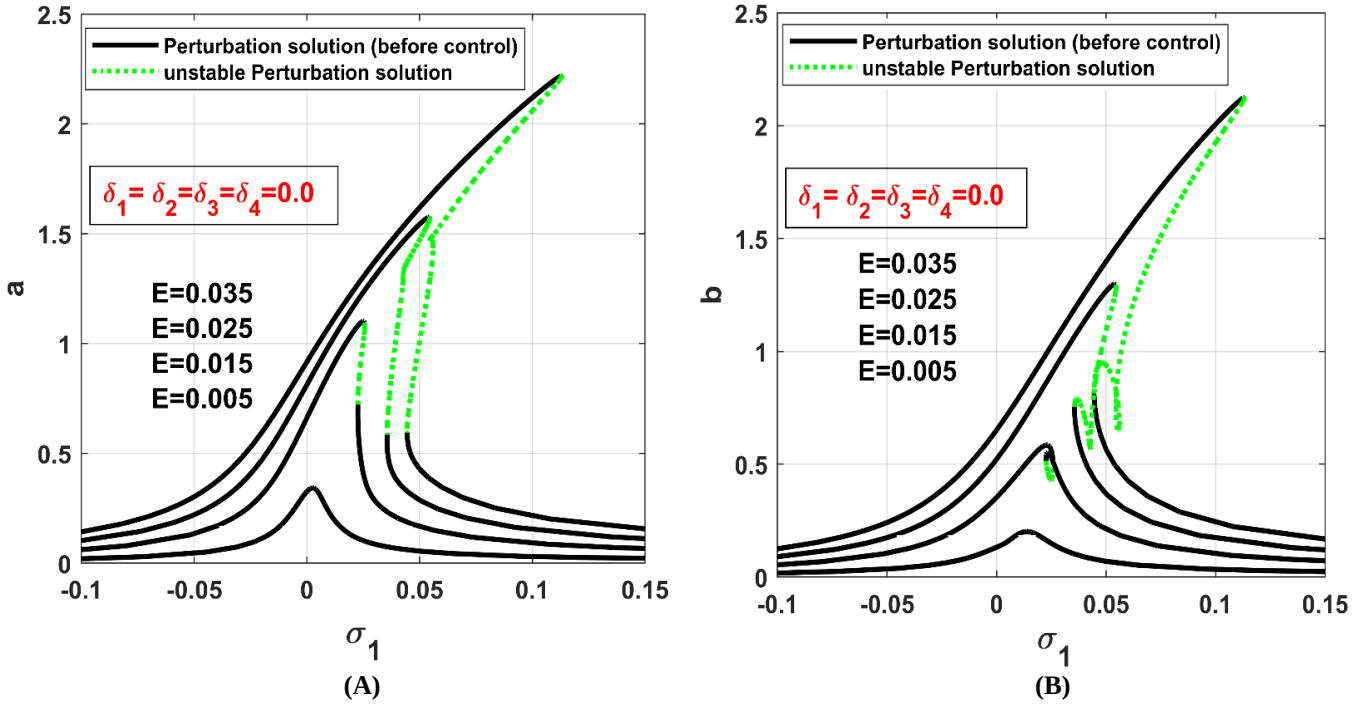

Figure 4. Steady-state vibration amplitudes of the rotor system before control at four different values of the excitation amplitude E: (A) Horizontal oscillation amplitude a against the parameter σ_1, and (B) Vertical oscillation amplitude b against the parameter σ_1.

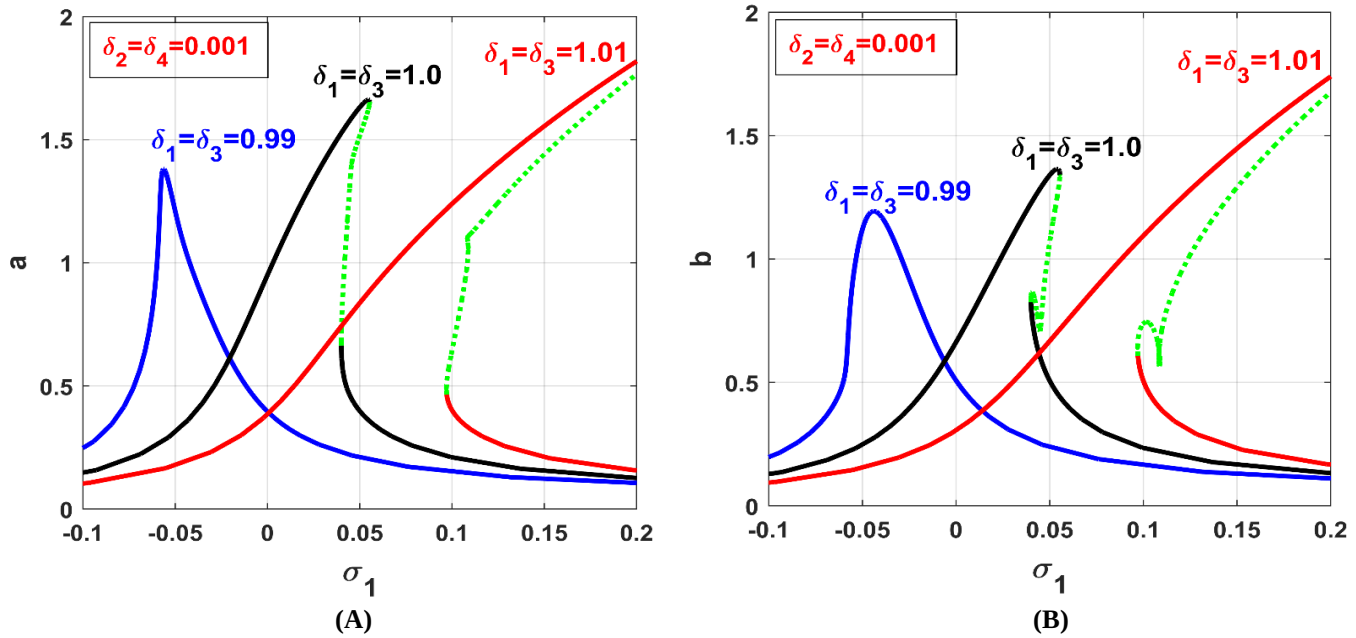

Figure 5. Steady-state vibration amplitudes of the rotor system after control at three different values of the proportional controller gains (i.e., $\delta_1 = \delta_3 = 0.99, 1.0, 1.01$) when $E = 0.035$, and $\delta_2 = \delta_4 = 0.001$: (A) Horizontal oscillation amplitude a against the parameter σ_1, and (B) Vertical oscillation amplitude b against the parameter σ_1.

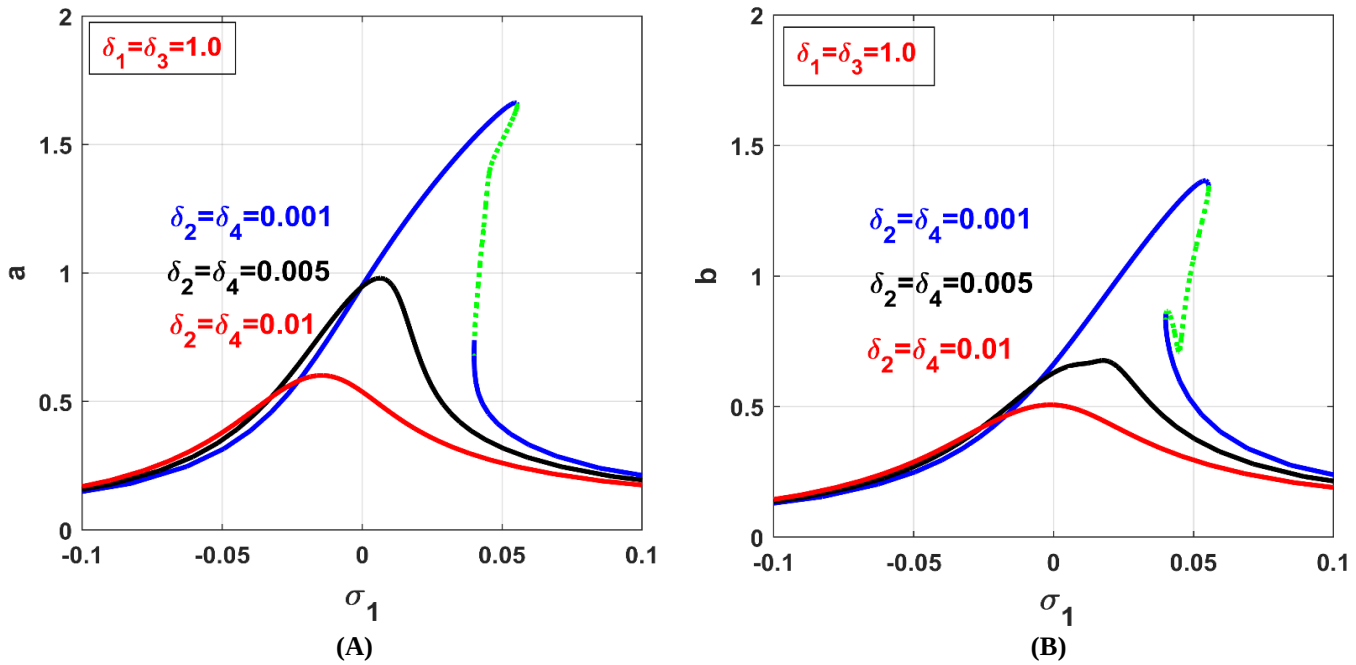

Figure 6. Steady-state vibration amplitudes of the rotor system after control at three different values of the integral controller gains (i.e., $\delta_2 = \delta_4 = 0.001, 0.005, 0.01$) when $E = 0.035$, and $\delta_1 = \delta_3 = 1.0$: (A) Horizontal oscillation amplitude a against the parameter σ_1, and (B) Vertical oscillation amplitude b against the parameter σ_1.

V. NUMERICAL VALIDATIONS AND SYSTEM DYNAMICS

The performance of the proposed controller in mitigating the undesired lateral vibration of the considered system has been explored within this section. In addition, numerical validations for the obtained results have been performed [41]. Figure (7) illustrates the steady-state vibrations amplitudes of the rotor system in both the horizontal direction (i.e., a) and the vertical direction (i.e., b) versus the parameter σ_1 before control (i.e., $\delta_1 = \delta_2 = \delta_3 = \delta_4 = 0$) and after control (i.e., $\delta_1 = \delta_3 = 1.0$, $\delta_2 = \delta_4 = 0.05$). Moreover, numerical validations for the obtained perturbation solution given by Equations (49)-(52) have been presented as small circles via solving the original equations of motion (i.e., Equations (20)-(32)) numerically using the Runge-Kutta algorithm. By examining Figure (7), one can deduce that the high oscillation amplitudes of the system before control at the resonance condition have been mitigated to a negligible amplitude after control. In addition, the system is forced to respond as a linear one, where the nonlinear characteristics such as the existence of multiple solutions and motion instability have been eliminated.

To validate the efficiency of the combined controller in mitigating the system vibration even at the large

excitation amplitude E, the steady-state vibration amplitudes before and after control have been plotted against E, where E is utilized as a bifurcation parameter as shown in Figure (8). It is clear from the figure that the oscillation amplitudes of the controlled system are smaller than that before control even at the large excitation force. Finally, the temporal oscillations of the system given by Equations (20)-(32) have been simulated before and after turning on the controller as shown in Figure (9). The figure simulates the system's temporal oscillations before control (i.e., $\delta_1 = \delta_2 = \delta_3 = \delta_4 = 0$) on the time interval $0 \le t < 800$, while the controller has turned on along the time interval $800 \le t \le 1000$ via setting $\delta_1 = \delta_3 = 1.0$ and $\delta_2 = \delta_4 = 0.05$ at the instant $t = 800$. It is clear from Figures (9A) and (9B) that the high temporal oscillations (in both the horizontal and vertical directions) before control on the interval $0 \le t < 800$ have been suppressed to very small temporal vibrations on the time interval $800 \le t \le 1000$ after control, where the excessive vibrations have been channeled to the controller as in Figures Figures (9C) and (9D).

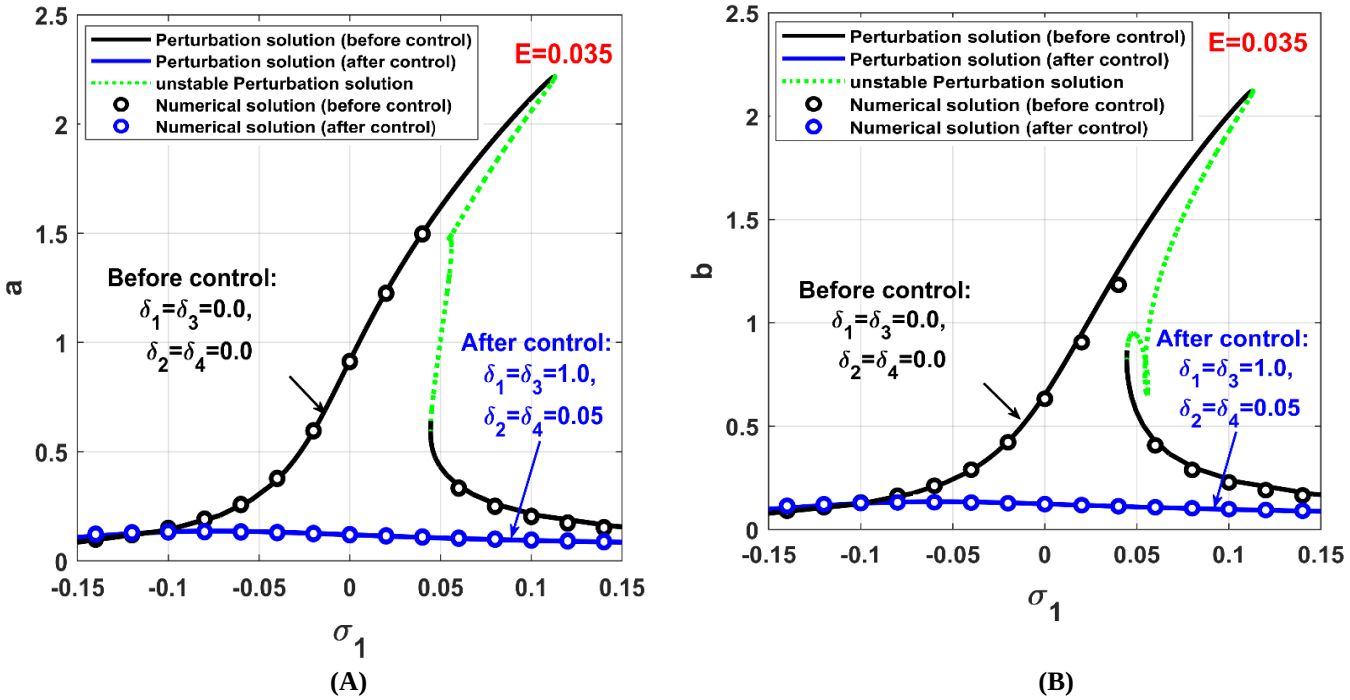

(A) **(B)**

Figure 7. Steady-state vibration amplitudes of the rotor system versus σ_1 before control (i.e., $\delta_1 = \delta_2 = \delta_3 = \delta_4 = 0.0$) and after control ($\delta_1 = \delta_3 = 1.0$, $\delta_2 = \delta_4 = 0.05$) when $E = 0.035$: (A) Horizontal oscillation amplitude a against the parameter σ_1, and (B) Vertical oscillation amplitude b against the parameter σ_1.

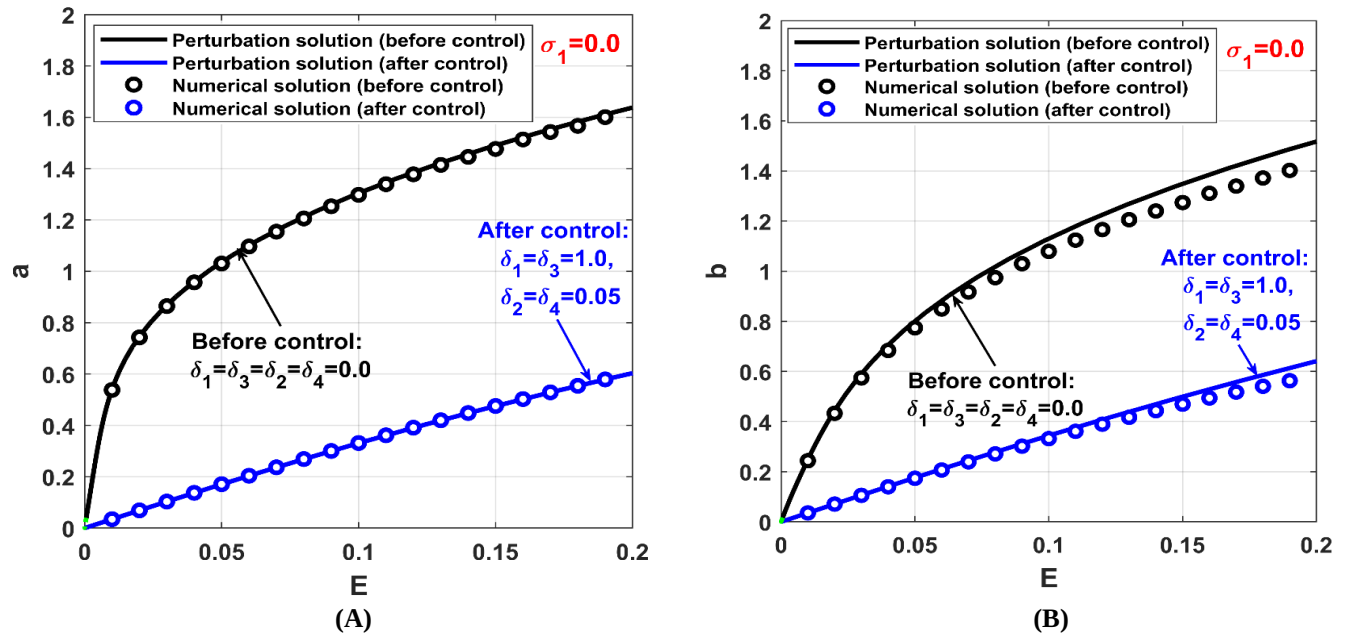

(A) **(B)**

Figure 8. Steady-state vibration amplitudes of the rotor system versus E before control (i.e., $\delta_1 = \delta_2 = \delta_3 = \delta_4 = 0.0$) and after control ($\delta_1 = \delta_3 = 1.0$, $\delta_2 = \delta_4 = 0.05$) when $\sigma_1 = 0.0$: (A) Horizontal oscillation amplitude a against the parameter σ_1, and (B) Vertical oscillation amplitude b against the parameter σ_1.

(A)

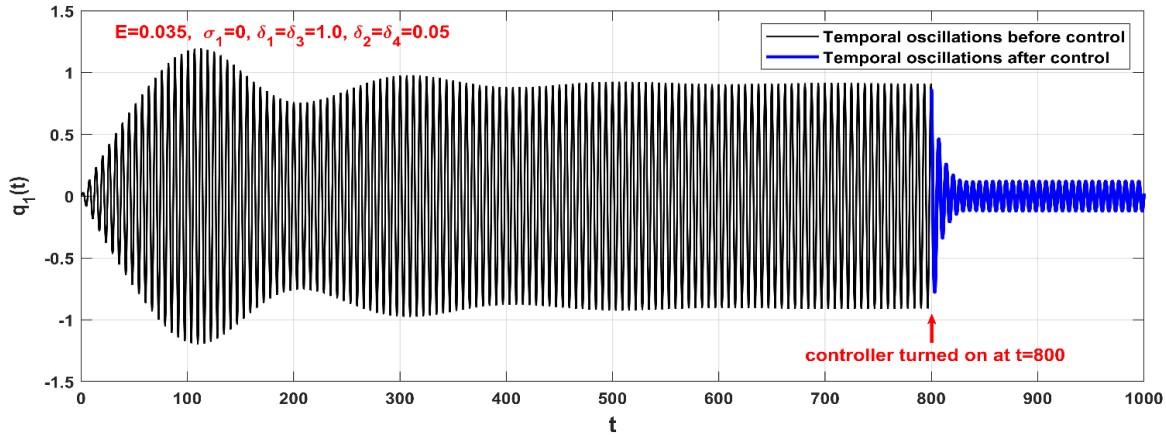
E=0.035, σ1=0, δ1=δ3=1.0, δ2=δ4=0.05
Temporal oscillations before control
Temporal oscillations after control
controller turned on at t=800
q1(t)
t

(B)

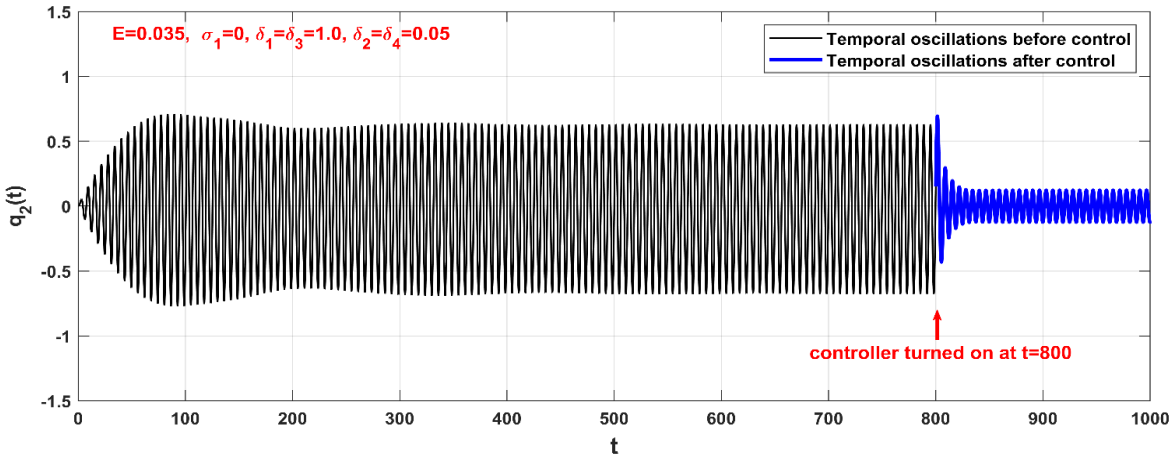
E=0.035, σ1=0, δ1=δ3=1.0, δ2=δ4=0.05
Temporal oscillations before control
Temporal oscillations after control
controller turned on at t=800
q2(t)
t

(C)

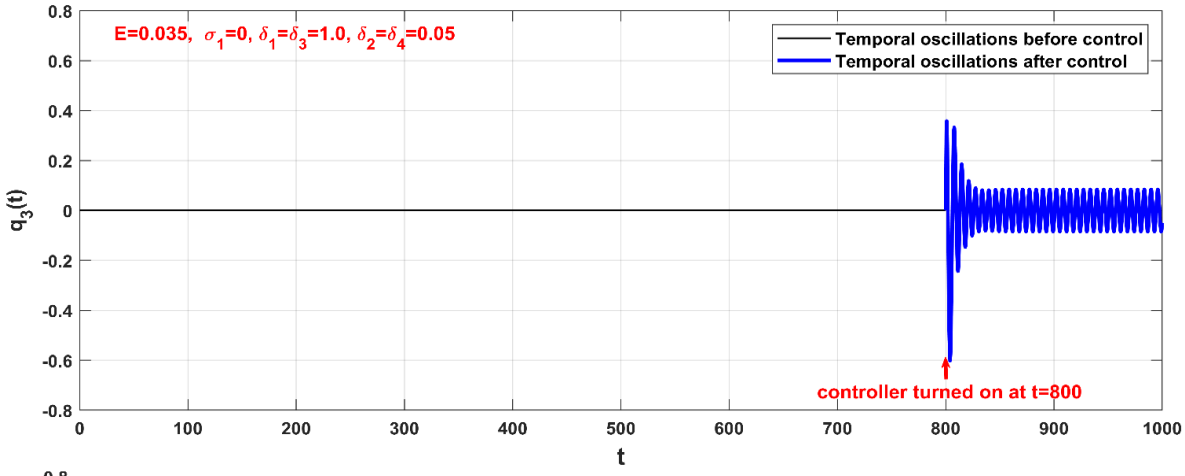
E=0.035, σ1=0, δ1=δ3=1.0, δ2=δ4=0.05
Temporal oscillations before control
Temporal oscillations after control
controller turned on at t=800
q3(t)
t

(D)

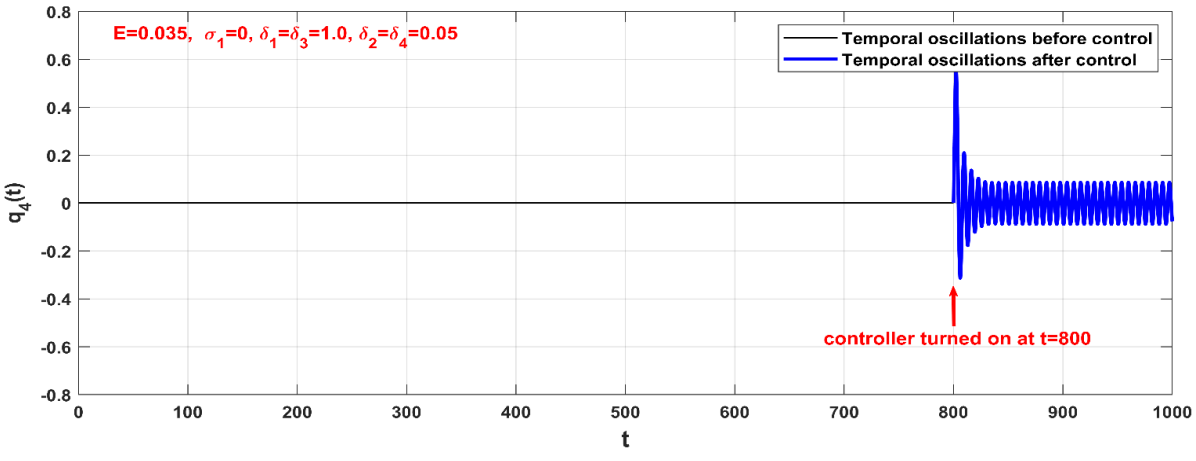
E=0.035, σ1=0, δ1=δ3=1.0, δ2=δ4=0.05
Temporal oscillations before control
Temporal oscillations after control
controller turned on at t=800
q4(t)
t

Figure 9. The system time response before control (i.e., $\delta_1 = \delta_2 = \delta_3 = \delta_4 = 0$) and after control (i.e., $\delta_1 = \delta_3 = 1.0,\ \delta_2 = \delta_4 = 0.05$) according to Figure (8) at $\sigma_1 = 0.0$: (A, B) Lateral vibration in the horizontal and vertical directions before and after control, and (C, D) The associated control signal of the integral resonant controller.

VI. CONCLUSIONS

The nonlinear vibration control of a horizontally suspended Jeffcott rotor system has been tackled within this paper using a combination of both the proportional and the integral resonant controllers. The proposed control technique has been integrated into the rotor system via an 8-pole active-magnetic bearing that acts as an actuator. The whole system mathematical model has been derived as two second-order nonlinear differential equations governing the lateral vibration of the rotor system, which are coupled to two first-order differential equations that govern the dynamics of the controller. The derived mathematical model has been normalized and then analyzed using the multiple-scale perturbation method up to the second-order approximation. The amplitude-phase modulation equations that govern the rotor vibration amplitudes and the corresponding phase angles terms of the system and controller parameters are obtained as four coupled nonlinear first-order autonomous systems. Based on the obtained amplitude-phase modulation equations, the effects of both the system and controller parameters on the system vibration amplitudes have been studied using different bifurcation diagrams. The main acquired results revealed the possibility of avoiding the rotor resonance frequency by changing the proportional controller gains δ_1 and δ_3. In addition, one can increase the system equivalent damping coefficients using the control gains of the integral resonant controller (i.e., δ_2 and δ_4), which ultimately eliminates the nonlinear characteristics and forces the system to respond as a linear one.

ACKNOWLEDGMENT

This work was also supported by the National Science Centre, Poland under grant number OPUS 14 No. 2017/27/B/ST8/01330.

REFERENCES

[1] Yamamoto, T. On the vibrations of a shaft supported by bearings having radial clearances. Trans. Jpn. Soc. Mech. Eng. **1955**, vol 21(103), pp.186–192.

[2] Ehrich, F.F. High-order subharmonic response of highspeed rotors in bearing clearance. ASME J. Vib. Acoust. Stress. Reliab. Des. **1988**, vol 110(1), pp.9–16.

[3] Ganesan, R. Dynamic response and stability of a rotor support system with non-symmetric bearing clearances. Mechanism and Machine Theory **1996**,vol 31(6),pp. 781–798.

[4] Yamamoto, T.; Ishida, Y. Theoretical discussions on vibrations of a rotating shaft with non-linear spring characteristics. Archive of Applied Mechanics **1977**,vol 46 (2),pp. 125-135.

[5] Ishida, Y.; Ikeda, T.; Yamamoto, T.; Murakami, S. Vibration of a rotating shaft with non-linear spring characteristics during acceleration through a critical speed. 2nd report. A critical speed of a 1/2-order subharmonic oscillation. Transactions of the japan society of mechanical engineers **1986**, vol 55(511-C),pp. 636-643.

[6] Ishida, Y.; Ikeda, T; Yamamoto, T.; Murakami, S. Nonstationary vibration of a rotating shaft with non-linear spring characteristics during acceleration through a critical speed. A critical speed of a 1/2-order subharmonic oscillation. JSME international journal **1989**, vol 32(4-III),pp. 575-584.

[7] Chávez, J. P.; Hamaneh, V. V.; Wiercigroch, M. Modelling and experimental verification of an asymmetric Jeffcott rotor with radial clearance, Journal of Sound and Vibration **2015**,pp. 334, 86-97.

[8] Saeed, N. A. On the steady-state forward and backward whirling motion of asymmetric nonlinear rotor system. European Journal of Mechanics - A/Solids 2020,vol 80, 103878.

[9] Adiletta, G.; Guido, A.R.; Rossi, C. Non-periodic motions of a Jeffcott rotor with non-linear elastic restoring forces. Non-linear Dyn **1996**,vol 11,pp. 37–59.

[10] Kim, Y.; Noah, S. Quasi-periodic response and stability analysis for a non-linear Jeffcott rotor. Journal of Sound and Vibration **1996**, vol 190(2),pp. 239-253.

[11] Han, Q.; Chu, F. Parametric instability of a Jeffcott rotor with rotationally asymmetric inertia and transverse crack. Non-linear Dyn **2013**,vol 73,pp. 827–842.

[12] Saeed, N.A., Eissa, M. Bifurcations of periodic motion of a horizontally supported nonlinear Jeffcott rotor system having transversely cracked shaft. International Journal of Non-Linear Mechanics 2018,vol 101,pp. 113-130.

[13] Saeed, N.A., Eissa, M. Bifurcation analysis of a transversely cracked nonlinear Jeffcott rotor system at different resonance cases. Int. J. Acoust. Vib. 2019,vol 24 (2),pp. 284-302

[14] Saeed, N.A.; Mohamed, M.S.; Elagan, S.K. Periodic, Quasi-Periodic, and Chaotic Motions to Diagnose a Crack on a Horizontally Supported Non-linear Rotor System. Symmetry 2020,vol 12, pp.2059.

[15] Chang-Jian, C.-W.; Chen, C.-K. Chaos of rub–impact rotor supported by bearings with non-linear suspension. Tribology International **2009**,vol 42, pp.426–439.

[16] Chang-Jian, C.-W.; Chen, C.-K. Non-linear analysis of a rub-impact rotor supported by turbulent couple stress fluid film journal bearings under quadratic damping. Non-linear Dyn **2009**,vol 56, pp.297–314.

[17] Khanlo, H.M.; Ghayour. M.; Ziaei-Rad, S. Chaotic vibration analysis of rotating, flexible, continuous shaft-disk system with a rub-impact between the disk and the stator. Commun Non-linear Sci Numer Simulat **2011**,vol 16,pp. 566–582.

[18] Chen, Y.; Liu, L.; Liu, Y.; Wen, B. Non-linear Dynamics of Jeffcott Rotor System with Rub-Impact Fault. Advanced Engineering Forum 2011,vol 2-3,pp.722-727.

[19] Wang, J.; Zhou, J.; Dong, D.; Yan, B.; Huang, C. Non-linear dynamic analysis of a rub-impact rotor supported by oil film bearings. Arch Appl Mech **2013**,vol 83,pp. 413–430.

[20] Khanlo, H.M.; Ghayour. M.; Ziaei-Rad, S. The effects of lateral–torsional coupling on the non-linear dynamic behavior of a rotating continuous flexible shaft–disk system with rub–impact. Commun Non-linear Sci Numer Simulat **2013**,vol 18,pp. 1524–1538.

[21] Hu, A.; Hou, L.; Xiang, L. Dynamic simulation and experimental study of an asymmetric double-disk rotor-bearing system with rub-impact and oil-film instability. Non-linear Dyn **2016**,vol 84,pp. 641–659.

[22] Eissa. M., Saeed, N. Nonlinear vibration control of a horizontally supported Jeffcott-rotor system. Journal of Vibration and Control. 2018, vol 24(24),pp. 5898-5921.

[23] Ishida, Y., Inoue, T.: Vibration Suppression of non-linear rotor systems using a dynamic damper. Journal of Vibration and Control vol 13(8),pp. 1127–1143 (2007).

[24] Saeed, N. A., Kamel, M. Nonlinear PD-controller to suppress the nonlinear oscillations of horizontally supported Jeffcott-rotor system. International Journal of Non-Linear Mechanics 2016,vol 87, pp. 109-124.

[25] Saeed, N.A.; El-Bendary, S.I.; Sayed, M.; Mohamed, M.S.; Elagan, S.K. On the oscillatory behaviours and rub-impact forces of a horizontally supported asymmetric rotor system under position-velocity feedback controller. Lat. Am. J. solids struct. 2021,vol 18, pp. e349.

[26] Saeed, N.A.; Awwad, E.M.; Maarouf, A.; Farh, H.M.H.; Alturki, F.A.; Awrejcewicz, J. Rub-impact force induces periodic, quasiperiodic, and chaotic motions of a controlled asymmetric rotor system. Shock. Vib. 2021, 1800022.

[27] Saeed, N.A., Awwad, E. M., EL-meligy, M. A., Abouel Nasr, E. Analysis of the rub-impact forces between a controlled nonlinear rotating shaft system and the electromagnet pole legs. Applied Mathematical Modelling 2021,vol 93,pp. 792-810.

[28] Ji, J.C. Dynamics of a Jefcott rotor-magnetic bearing system with time delays. International Journal of Non-Linear Mechanics **2003**, vol 38, pp. 1387 – 1401.

[29] El-Shourbagy, S. M.; Saeed, N.A.; Kamel, M.; Raslan, K.R.; Abouel Nasr, E.; Awrejcewicz, J. On the Performance of a Non-linear Position-Velocity Controller to Stabilize Rotor-Active Magnetic-Bearings System. Symmetry **2021**,vol 13, 2069.

[30] Saeed, N.A.; Awrejcewicz, J.; Mousa, A.A.A.; Mohamed, M.S. ALIPPF-Controller to Stabilize the Unstable Motion and Eliminate the Non-Linear Oscillations of the Rotor Electro-Magnetic Suspension System. Appl. Sci. **2022**, vol 12, 3902.

[31] Saeed, N.A.; Mohamed, M.S.; Elagan, S.K.; Awrejcewicz, J. Integral Resonant Controller to Suppress the Non-linear Oscillations of a Two-Degree-of-Freedom Rotor Active Magnetic Bearing System. Processes **2022**,vol 10, 271.

[32] Saeed, N. A.; Awwad, E. M.; El-Meligy, M. A.; Nasr, E. S. A. Radial versus cartesian control strategies to stabilize the non-linear whirling motion of the six-pole rotor-AMBs. IEEE Access **2020**,vol 8,pp. 138859-138883.

[33] El-Shourbagy, S.M.; Saeed, N.A.; Kamel, M.; Raslan, K.R.; Aboudaif, M.K.; Awrejcewicz, J. Control Performance, Stability Conditions, and Bifurcation Analysis of the Twelve-Pole Active Magnetic Bearings System. Appl. Sci. **2021**,vol 11, 10839.

[34] Saeed, N.A., Omara, O.M., Sayed, M. et al. On the rub-impact force, bifurcations analysis, and vibrations control of a nonlinear rotor system controlled by magnetic actuator integrated with PIRC-control algorithm. SN Appl. Sci 2023, 5, 41.

[35] Ishida, Y.; Yamamoto, T. Linear and Non-linear Rotordynamics: A Modern Treatment with Applications, 2nd ed.; Wiley-VCH Verlag GmbH & Co. KGaA: New York, NY, USA, 2012.

[36] Schweitzer, G.; Maslen, E.H. Magnetic Bearings: Theory, Design, and Application to Rotating Machinery; Springer: Berlin/Heidelberg, Germany, 2009.

[37] Nayfeh, A.H.; Mook, D.T. Non-linear Oscillations; Wiley: New York, NY, USA, 1995.

[38] Nayfeh, A.H. Resolving Controversies in the Application of the Method of Multiple Scales and the Generalized Method of Averaging. Non-linear Dyn vol 40, pp. 61–102 (2005).

[39] Saeed, N.A., Moatimid, G.M., Elsabaa, F.M.F. et al. Time-delayed control to suppress a nonlinear system vibration utilizing the multiple scales homotopy approach. Arch Appl Mech 91,pp. 1193–1215, (2021).

[40] Saeed, N. A., Moatimid, G. M., Elsabaa, F. M., Ellabban, Y. Y., Elagan, S. K., Mohamed, M. S. Time-Delayed Nonlinear Integral Resonant Controller to Eliminate the Nonlinear Oscillations of a Parametrically Excited System. IEEE Access 2021,vol 9,pp. 74836-74854.

[41] Yang, W. Y.; Cao, W.; Chung, T.; Morris, J. Applied numerical methods using matlab. John Wiley & Sons, Inc., Hoboken, New Jersey, Canada, 2005.